LA-12669-MS

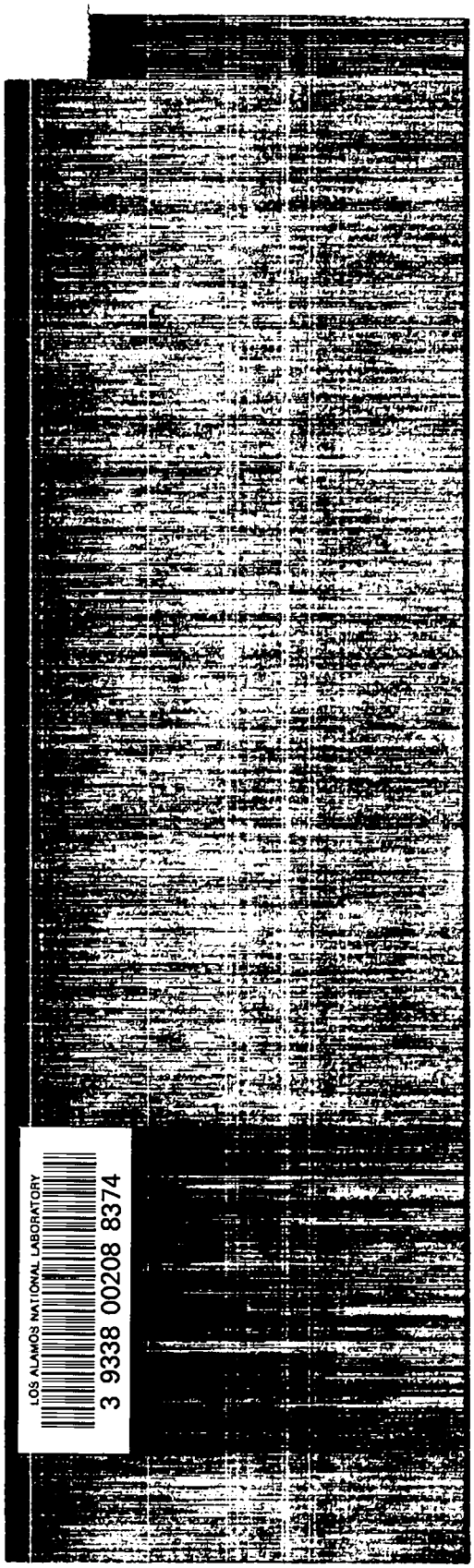

Constitutive Equations for Annealed Metals Under Compression at High Strain Rates and High Temperatures

Los Alamos
NATIONAL LABORATORY

Los Alamos National Laboratory is operated by the University of California for the United States Department of Energy under contract W-7405-ENG-36.

Edited by Pat Wing, Group IS-1

This work was jointly supported by the US Army Block Funding program under a Memorandum of Understanding between the US Army, the US Department of Energy, and the DARPA-US Army-US Marine Corps Joint Program Office.

Document coordinated and reviewed for classification by S. R. Skaggs, Derivative Classifier and Armor Program Manager, Los Alamos National Laboratory, under Sections VI and VII of the Warheads and Warhead Technology Security Classification Guide, published 15 October 1992, Wright Laboratory (AFMC) Armament Directorate, Eglin AFB, FL 32542-5434.

An Affirmative Action/Equal Opportunity Employer

LA-12669-MS

UC-000
Issued: January 1994

Constitutive Equations for Annealed Metals Under Compression at High Strain Rates and High Temperatures

G. T. Gray III
Shuh Rong Chen
W. Wright
M. F. Lopez

Los Alamos
NATIONAL LABORATORY
Los Alamos, New Mexico 87545

CONSTITUTIVE EQUATIONS FOR ANNEALED METALS UNDER COMPRESSION AT HIGH STRAIN RATES AND HIGH TEMPERATURES

by

G. T. Gray III, Shuh Rong Chen, W. Wright, and M. F. Lopez

ABSTRACT

Several metals were subjected to split Hopkinson pressure bar loading in compression to determine the stress-strain relationship over a wide range of temperatures and strain rates. Metals examined in this series of tests include 4340 steel with a tempered martensite structure, rolled homogeneous armor (RHA) steel, tantalum, OFE copper, Al-7039, and Al-5083. The range of temperatures varied from –196°C to 600°C. The strain rates ranged from a quasistatic value of 0.001/s to a very high rate of 7000/s. Curves are presented for each and fits are made using the Johnson-Cook or the Zerilli-Armstrong constitutive material model. The constants for each model are shown at the bottom of each graph to allow readers to assess the fairness of fit and choose the most applicable set of curves for their calculations.

INTRODUCTION

Modeling materials undergoing high rate deformation has been of great interest to the materials science community for many years. The availability of modern computers allows us to develop codes to model complex problems (e.g., plate perforation by a shaped charge jet, cylinder impact into massive targets, etc.). In great demand are both an accurate description of the material properties and having predictive capability outside the measured range. Two models used particularly for high-strain-rate applications are the Johnson-Cook (JC) model[1] and the Zerilli-Armstrong (ZA) model.[2] With large scale predictive computations in mind, these investigators have succeeded in developing simple, easy to use forms of constitutive equations. We report data for several materials over a wide range of strain rates by fitting with these two models, and a modified Zerilli-Armstrong (MZA) model by Goldthorpe,[3] which uses temperature dependence in a form corrected by the shear modulus. Data are presented in a series of figures with the model parameters shown at the bottom of the page.

DATA ANALYSIS

Data on the materials tested were obtained using a Split Hopkinson pressure bar in compression for strain rates at several thousands per second. The Split Hopkinson pressure bar facility is equipped with a vacuum furnace to perform high-rate tests up to 1200°C. The low-rate data were taken using either an Instron or an MTS testing system. Metals examined in this series of tests include 4340 steel with a tempered martensitic structure, rolled homogeneous armor (RHA) steel, tantalum, OFE copper, Al-7039 and Al-5083. Pertinent technical data on the materials are included in Appendix B.

The constitutive equations used in this study are in the following forms.

Johnson-Cook Model:[1]

$$\sigma = (A + B \cdot \varepsilon^n)(1 + C \ln \dot{\varepsilon}^*)(1 - T^{*m}) \tag{1}$$

$\dot{\varepsilon}^*$ is a non-dimensional strain rate value. The original form of T^* is $(T - T_{ROOM})/(T_{MELT} - T_{ROOM})$. In our data analysis, we use the original form to fit data above room temperature and use $T^* = T/T_{MELT}$ if data below room temperature are included; T is in degrees Kelvin.

Zerilli-Armstrong Model:[2]

$$\sigma = C_0 + C_1 \exp(-C_3 T + C_4 T \cdot \ln \dot{\varepsilon}) + C_5 \varepsilon^n \qquad \text{(BCC)} \tag{2}$$

$$\sigma = C_0 + C_2 \varepsilon^n \exp(-C_3 T + C_4 T \cdot \ln \dot{\varepsilon}) \qquad \text{(FCC)} \tag{3}$$

and Modified Zerilli-Armstrong Model:

$$\sigma = C_0 + C_1 \exp(-C_3 T + C_4 T \cdot \ln \dot{\varepsilon}) + (C_5 \varepsilon^n + C_6)\frac{\mu(T)}{\mu_{293}} \quad \text{(BCC)} \tag{4}$$

$$\sigma = C_0 + C_2 \varepsilon^n \exp(-C_3 T + C_4 T \cdot \ln \dot{\varepsilon})\frac{\mu(T)}{\mu_{293}} \qquad \text{(FCC)} \tag{5}$$

One observation in the JC model on the use of T^* needs to be addressed in detail. In the paper by Johnson and Cook,[1] they used

$$T^* = (T - T_{ROOM})/(T_{MELT} - T_{ROOM}) \tag{6}$$

and called it the homologous temperature. The disadvantage in using this definition for temperature is that the model can not be applied to test data below room temperature. Secondly, it does not really correspond to *the homologous temperature that is defined as the temperature with respect to the absolute melting temperature.*

$$T^* = T/T_{MELT} \tag{7}$$

This definition of homologous temperature has been widely used in recrystallization (for example, see [4]) and has served as a rough demarcation of certain material properties. In recent papers by Johnson *et al.*,[5, 6] they used the same definition for T^* with the explicitly written form of T^* in [5] and without the form in [6], but in both papers they called it the homologous temperature. Furthermore, we found that it was not necessary to subtract the value of room temperature before fitting the JC model.

For each model, programs were developed to solve the equations according to the methods described in references 1 and 2. Once this had been done, the range of corresponding constants is developed by comparing calculations at a given strain rate with the experimental data at that strain rate. This process is repeated for every curve we want to fit until a good agreement is found. A computer program which performs an optimization routine to fit the digitized data was developed. The time required to do several million calculations is only on the order of minutes using a personal computer. A parameter indicating the degree of fit is defined as

$$\delta = \frac{\sum_{i=1}^{n} \frac{\left|\sigma_{calculated}(\varepsilon_i) - \sigma_{experimental}(\varepsilon_i)\right|}{\sigma_{experimental}(\varepsilon_i)}}{n} \,. \tag{8}$$

Two points representing the characteristic hardening behavior on each stress-strain curve were taken to compare to the calculated stresses at the corresponding strain values. The deviation parameter for all the model fits presented is better than 2% except for Al alloys where it is slightly greater than 5%. The raw data for the materials used (4340, RHA, tantalum, OFE copper; Al-7039, and Al-5083) are given in Appendix A.

FIGURES AND DISCUSSION

Figures 1 and 2 show the data fits using the JC model for 4340 and RHA steels, respectively. The homologous temperature (T/T_{MELT}) (Eq. 7) is used for T^* in these fits. The JC model fits the data well for the high strain rate data over a range of temperature from boiling liquid nitrogen to about 600°C. All the models have been optimized to the high-rate data because it is felt these strain rate levels are most relevant to the applications of interest. Above 600°C, the material loses its tempered structure. The stress level at 800°C that is shown in Appendix A is very low.

Figure 3 shows the model fitting using the same method as in Figure 2 except the data were above room temperature. Here we strive to maintain the same magnitude strain rate sensitivity as that derived from data taken at liquid nitrogen temperature at both high and low strain rates. The fit is slightly better for the tests at 400°C and 600°C. If we allow the rate-sensitivity term, m, to vary in order to fit the data at room temperature at 7000/s and 3500/s (Fig. 3), then the constant C is more than ten times higher than the data of liquid nitrogen suggests. The results of using the original formula for temperature in the JC model for 4340 and RHA are shown in Figs. 3 and 4. In principle, it gives the same result for both temperature definitions. We will discuss these results later in the report. A similar argument on rate sensitivity is shown for comparison in Fig. 3a and Fig. 4a.

We did a thorough model fitting using the same method and all the data available on Al-7039 and Al-5083 alloys. Figures 5–16 are the results after fitting. Figure 5 shows the fitting for low- and high-rate data from liquid nitrogen temperature to 200°C. As shown in this figure, if we attempt to fit all the data using the JC model, the results are not very promising. *It raises a concern that one should exercise utmost care in extrapolating the model constants beyond that derived for a particular range of data.*

Figure 6 shows the result as in Figure 5 but only fitting with the high-rate data. The fit is improved. If we examine the experimental data, the stress level for 200°C is much lower than that suggested from the difference between the room temperature and the 100°C test. The microstructure of Al-7039 after deformation will be investigated to elucidate the cause of the stress drop at higher temperatures.

Figure 7 reveals the model fitting for all data above room temperature. The same procedure was taken for the fitting in Figure 8 but with the original temperature definition. High-rate data above room temperature were fitted using both temperature definitions on Al-7039 in Figures 9 and 10. One lesson that we learned here was that by fitting the JC model using a different range of data

we could obtain quite different model constants; compare values of the constants on Figures 7–10. We have to make a judgment decision in order to choose the appropriate range for data fitting. *Most importantly, we can not rely on only a few tests to derive the model constants.*

The same sequential approach was taken to fit the data for Al-5083 (Figures 11–16). The tests that were done at room temperature indicate that dynamic strain aging occurred because the stress level of the strain rate of 0.1/s is lower than that of 0.001/s (see the raw data on the figure for Al-5083 in Appendix A). It is probably due to Mg solute present in this alloy. The fitting as shown in Figure 11 for all data of Al-5083 is not good. On the contrary the fit for the four tests done at high rate and above room temperature in Figure 15 is excellent.

Figure 17 shows curves plotting the third term $(1 - T^{*}_{m})$ in the JC model versus the temperature using both definitions. The curve with open circles uses $T^{*} = T/T_{MELT}$ with m = 0.75 for 4340 steel. If we do another calculation with the same parameter m, but using $T^{*} = (T - T_{ROOM})/(T_{MELT} - T_{ROOM})$, then the dotted line is the result. This line shows a different temperature dependence especially if the temperature is less than 500 K. Adjustment of m is therefore necessary to have the same temperature dependence; the result is shown as the solid line in this figure. In order to bring the open circles coincident with the solid line, we only need to multiply the ordinates by 1.33; that is shown as the solid circles. Basically, these two definitions of T^{*} could have the identical curve fitting but with a different m and a constant ratio between the two sets of constants in A and B.

One example is shown in Figure 18. With a different m used to preserve the same temperature dependence and a factor of 1.33 between two sets of A and B, n and C could be kept the same; the fit indicated by the open circles and the solid triangles is essentially identical. This implies that we shall use $T^{*} = T/T_{MELT} \equiv$ homologous temperature instead of $T^{*} = (T - T_{ROOM})/(T_{MELT} - T_{ROOM}) \neq$ homologous temperature. However all four materials were fitted using both temperature definitions. We felt that the tests done at lower temperatures were meaningful in the sense that they give us an indication of how much the materials can strengthen. Therefore we should not ignore the importance of the upper bound. The only advantage in using the original temperature definition is that the value of A is close to the yield stress of the test at room temperature. In this case we suggest that it be called normalized temperature instead of homologous temperature.

Figures 19–24 are the fitting results using the ZA model for 4340 and RHA steels, tantalum, copper, Al-7039, and Al-5083. The JC model failed to yield a reasonable fit on copper

that we tested at high rate. The high dependence of stress on the strain hardening, as indicated by the divergence of stress at higher strains, was the cause. Figures 25–29 are obtained using the MZA model. (There is no modified ZA fit for tantalum.) The shear modulus corrected temperature dependence of the stresses in the MZA model is seen to give a slightly better fit to the data in general.

It is interesting to examine the curve fitting found in the literature. Figure 30 shows one example for 4340 steel taken from [1]. The corresponding set of constants accurately reproduces the curve for the test at 450°C and 650/s but not as well for the other two curves. Figure 31 shows the stress-strain curves for high hard armor (HHA) by Johnson and Holmquist.[7] The curves accurately fit the room temperature data but the accuracy at other temperatures is debatable. This set of constants fits our current 4340 tempered steel data reasonably well for the room temperature high-rate test (Figure 32). This implies that the HHA used in their study is very similar microstructurally to the 4340 steel we tested. As we mentioned above, the temperature dependence of their fit could be altered. If we emphasize it a little more so we have a better fit in terms of the test temperature (changing m from 1.17 to 0.9), then the fit is still within their data range. In this case, it fits well for the curves at 21°C and at 550°C (Figure 33). Using this set of constants to fit our data again, the stress level for each test condition is now satisfactory (Figure 34). However, the strain hardening rate is lower than the high-rate data shows. Their curve fitting captured more of the behavior of the low-rate test as can be seen in Figure 35 (10^{-3}/s for 4340 steel). *Again it emphasizes that extrapolation of data outside the measured range must be done carefully. This brings us to a recommendation that the data fit using any model should always be plotted with the experimental curves.* We have supplied the experimental curves as Appendix material so the reader can make an individual judgment. We have also presented the results of all of the various fits of the curves together with their constants. This will allow potential users to judge how good the fit of the constitutive equations is and to what extent it can be extrapolated.

Figure 35 compares the four different kinds of steels we have assembled in this study on one set of axes. The HHA characterized by Johnson and Holmquist is very similar to our 4340 tempered steel. The 4340 steel Johnson and Cook studied in 1983 had a very low stress level that indicates that it was probably annealed and cooled very slowly or might be quenched and then tempered at high temperature. The RHA steel we tested is different from both. In a recent discussion with Raftenberg at U.S. Army Ballistic Research Laboratory, he studied the plate perforation on RHA.[8] He observed that the hardness on the surfaces of the RHA used were, in Brinell hardness, 364 for a 1/2-in. plate, 320 for a 1-in. plate, and 300 for a 2-in. plate. The strength of the 1/2-in. RHA plate is close to the value for the steel we tested, but the strength of

2-in. plate is closer to the 4340 JC used. Therefore it is very important to give a stress strain curve at low temperature (e.g., room temperature) and at low strain rate (e.g., 10^{-3}/s). Before choosing the set of constants to use in calculations, one should do a simple test to verify the similarity between the material used in generating these constants and the material that will be used in the study of interest.

CONCLUSIONS AND FUTURE WORK

The models we have examined adequately describe our high-strain-rate data, but fail to describe the whole spectrum of all the test data (from liquid nitrogen temperature to high temperatures, and from low strain rates to high strain rates, as shown in Appendix A). We have presented our interpretation of the data based on selection of several temperatures and strain rates. The simplicity of the model is its merit, but that also limits its capability to handle more complex material behavior (for instance, the Peierls' stress contribution found for pure BCC material at low temperatures, the dynamic strain aging encountered in several engineering materials, and twinning which occurs at low temperatures and at high rates, etc.). A constitutive description of the deformation of copper at strain rates from 10^{-4} to 10^{4}/s has been successfully developed by Follansbee and Kocks[9] based on the use of the mechanical threshold stress as an internal state variable (MTS model). This model has been extended to other FCC materials as well as some BCC materials. Fitting our data using their model and comparing them with the results obtained using the models in this study is in progress.

REFERENCES

[1] G.R. Johnson and W.H. Cook, "Proceedings of the Seventh International Symposium on Ballistics," The Hague, The Netherlands, 1983, p. 541.

[2] F.J. Zerilli and R.W. Armstrong, J. Appl. Phys, 61(5), 1 March 1987, p. 1816.

[3] B.D. Goldthorpe, J. DE PHYSIQUE IV, October 1991, p. C3-829.

[4] G. Gottstein and U.F. Kocks, Acta Metall., vol. 31, 1983, p. 175.

[5] G.R. Johnson and W.H. Cook, Engineering Fracture Mechanics, vol. 21, 1985, p. 31.

[6] T.J. Holmquist and G.R. Johnson, J. DE PHYSIQUE IV, October 1991, p. C3-853.

[7] G.R. Johnson and T.J. Holmquist, "Test Data and Computational Strength and Fracture Model Constants for 23 Materials Subject to Large Strains, High Strain Rates, and High Temperatures," LA-11463-MS, Los Alamos National Laboratory, 1989, p. 1.

[8] M.N. Raftenberg, "Modeling RHA Plate Perforation by a Shaped Charge Jet," Technical Report BRL-TR-3363, Ballistic Research Laboratory, June 1992, p. 1.

[9] P.S. Follansbee and U.F. Kocks, Acta Metall., vol. 36, 1988, p. 81.

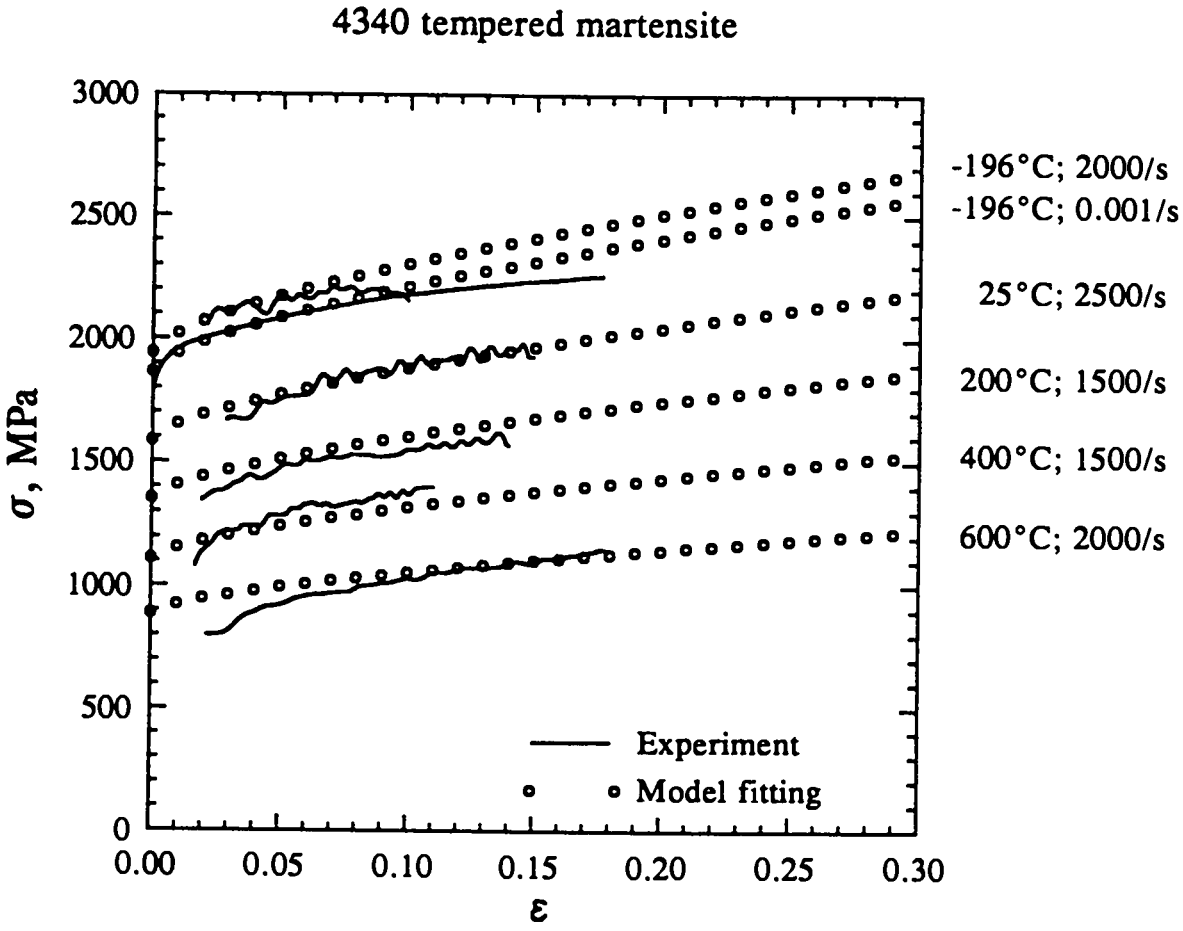

Johnson-Cook Model:

$$\sigma = (A + B\varepsilon^{n})(1 + C\ln\dot{\varepsilon}^{*})(1 - (T/T_m)^{m})$$

A=2100 MPa B=1750 MPa n=0.65

C=0.0028 m=0.75 T_m=1783 K

Figure 1. Fit of 4340 steel using the Johnson Cook equations using T* as in Eq. 7.

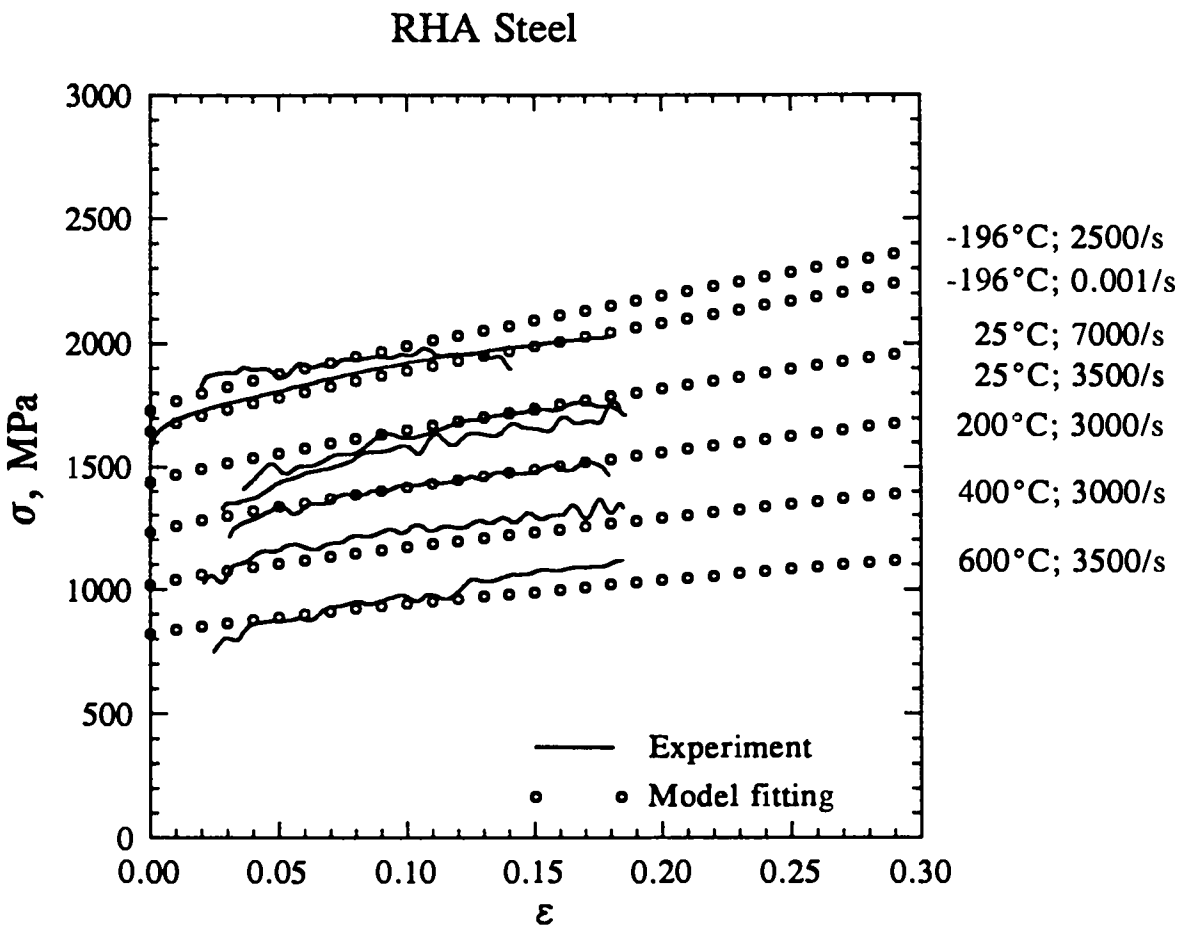

Johnson-Cook Model:

$$\sigma = (A + B\varepsilon^{n})(1 + C\ln\dot{\varepsilon}^{*})(1-(T/T_m)^{m})$$

A=1832 MPa B=1685 MPa n=0.754

C=0.00435 m=0.80 T_m=1783 K

Figure 2. Fit of RHA steel using the Johnson Cook equations using T* as in Eq. 7.

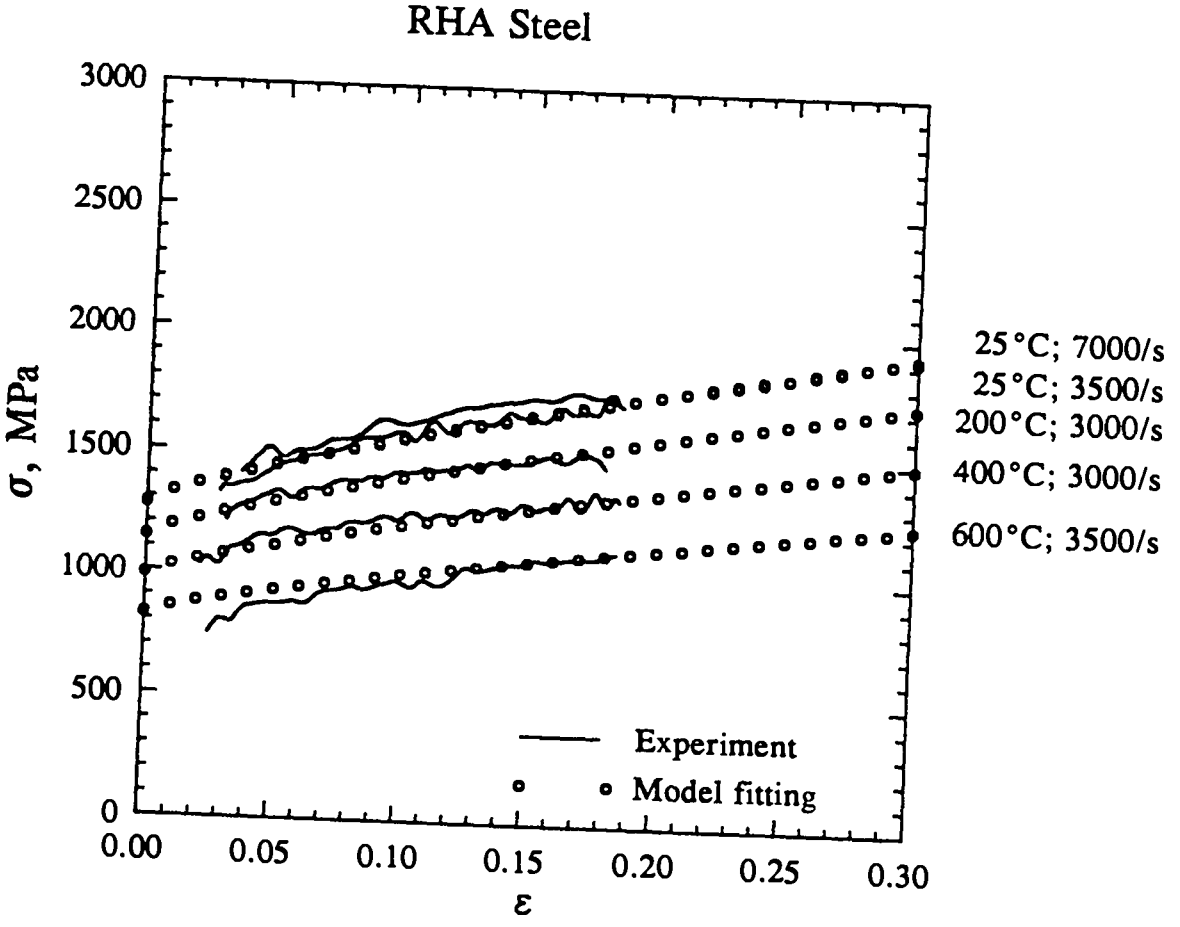

Johnson-Cook Model:

$$\sigma = (A + B\varepsilon^{n})(1 + C\ln\dot{\varepsilon}^{*})(1-(T/T_m)^{m})$$

A=1400 MPa B=1800 MPa n=0.768

C=0.0049 m=1.17 T_m=1783 K

Figure 3. Fit of RHA steel using the Johnson Cook and the homologous temperature T*.

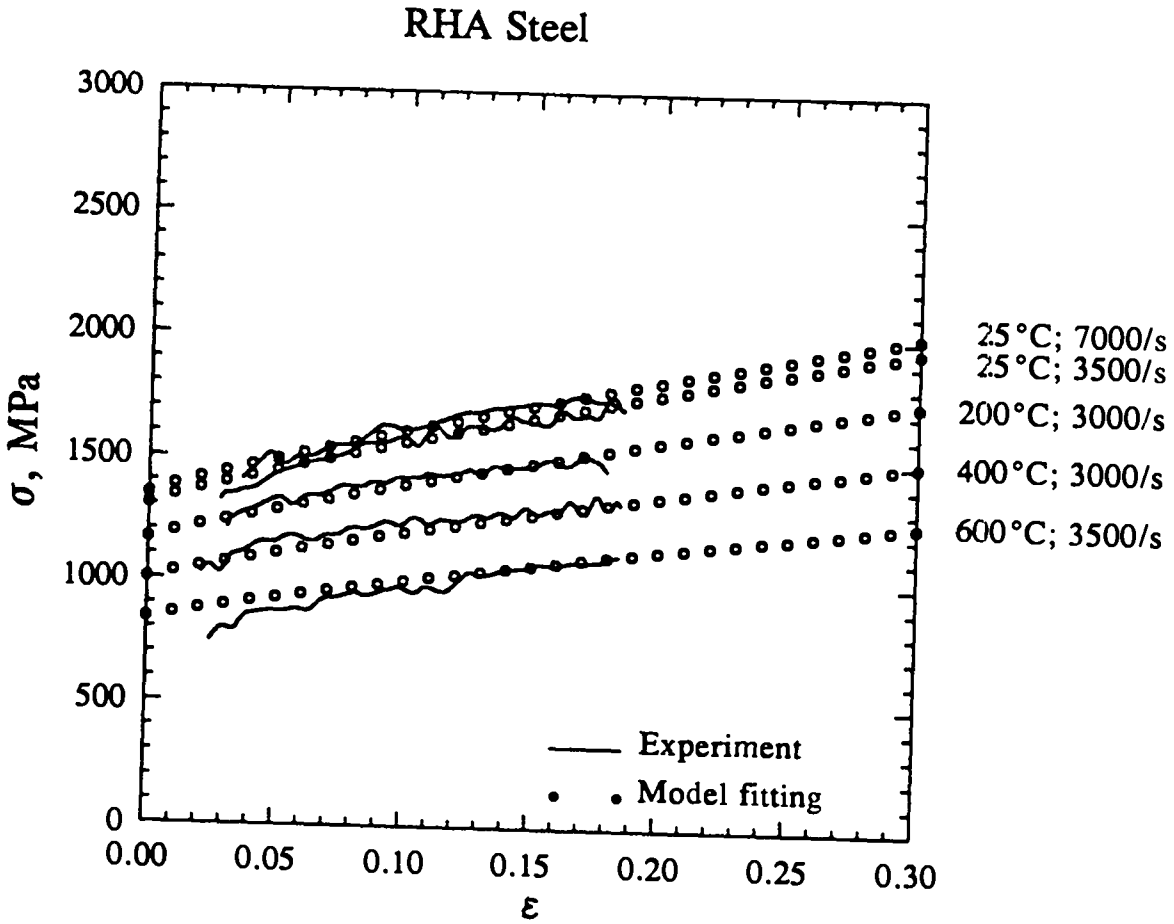

Johnson-Cook Model:

$$\sigma = (A + B\varepsilon^{n})(1 + C\ln\dot{\varepsilon}^{*})(1-(T/T_m)^{m})$$

A=960 MPa B=1330 MPa n=0.85

C=0.06875 m=1.15 T_m=1783 K

Figure 3a. Fit of RHA steel with high strain rate data using JC equations referencing RT.

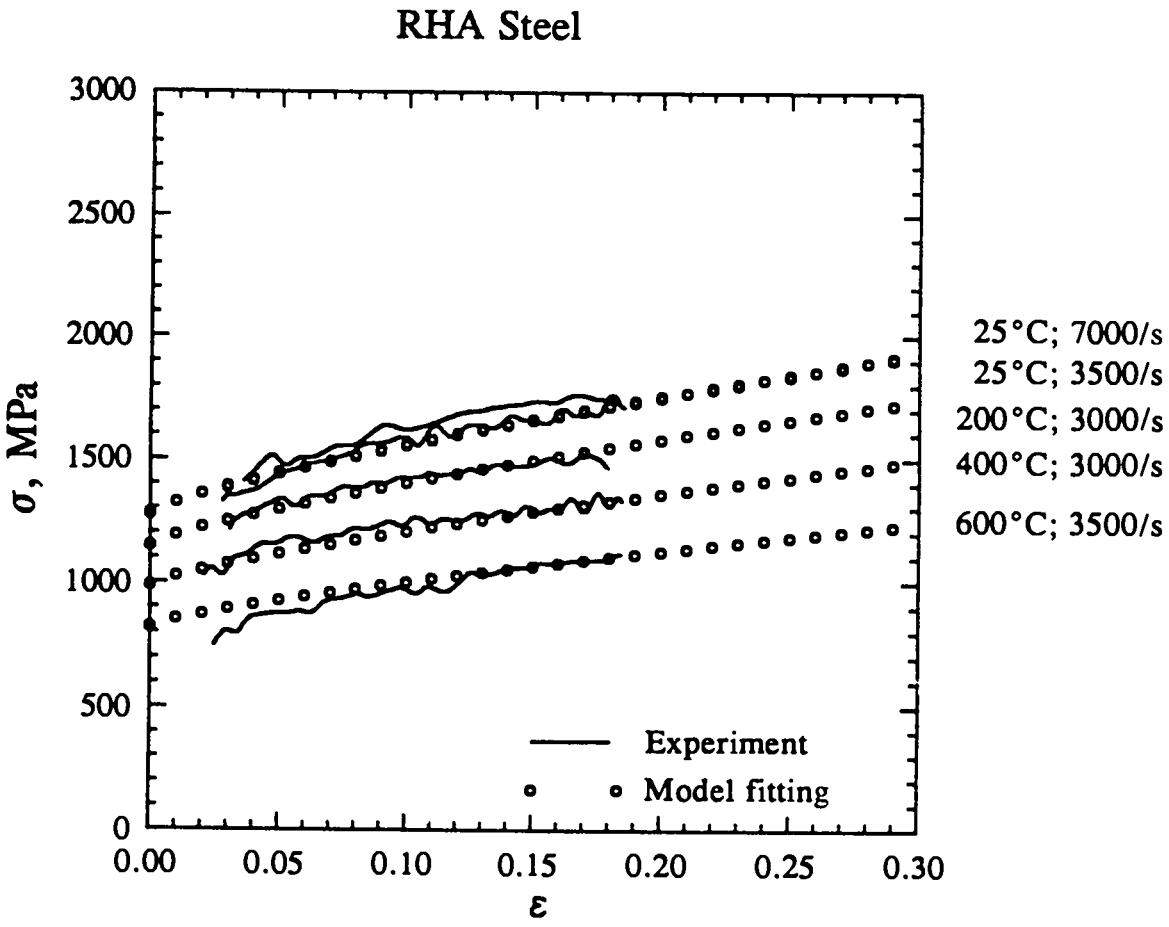

Johnson-Cook Model:

$$\sigma = (A + B\varepsilon^{n})(1 + C\ln\dot{\varepsilon}^{*})(1 - ((T - 298)/(T_m - 298))^{m})$$

A=1225 MPa B=1575 MPa n=0.768

C=0.0049 m=1.09 T_m=1783 K

Figure 4. Fit of RHA steel using the Johnson Cook equations referencing to room temperature.

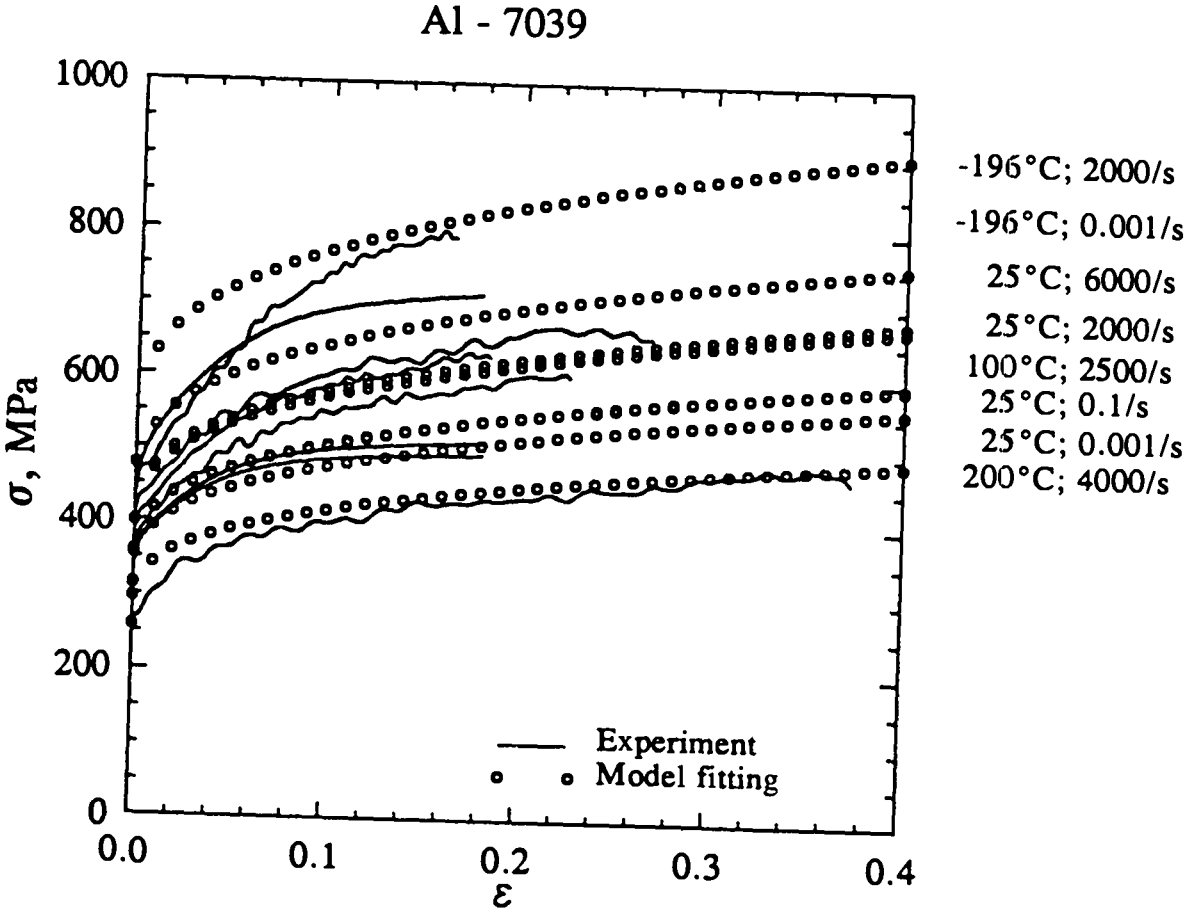

Johnson-Cook Model:

$$\sigma = (A + B\varepsilon^{n})(1 + C\ln\dot{\varepsilon}^{*})(1 - (T/T_{m})^{m})$$

A=475 MPa B=550 MPa n=0.275

C=0.0125 m=1.0 T_m=933 K

Figure 4a. Fit of RHA steel with high strain rate data using JC equations referencing RT.

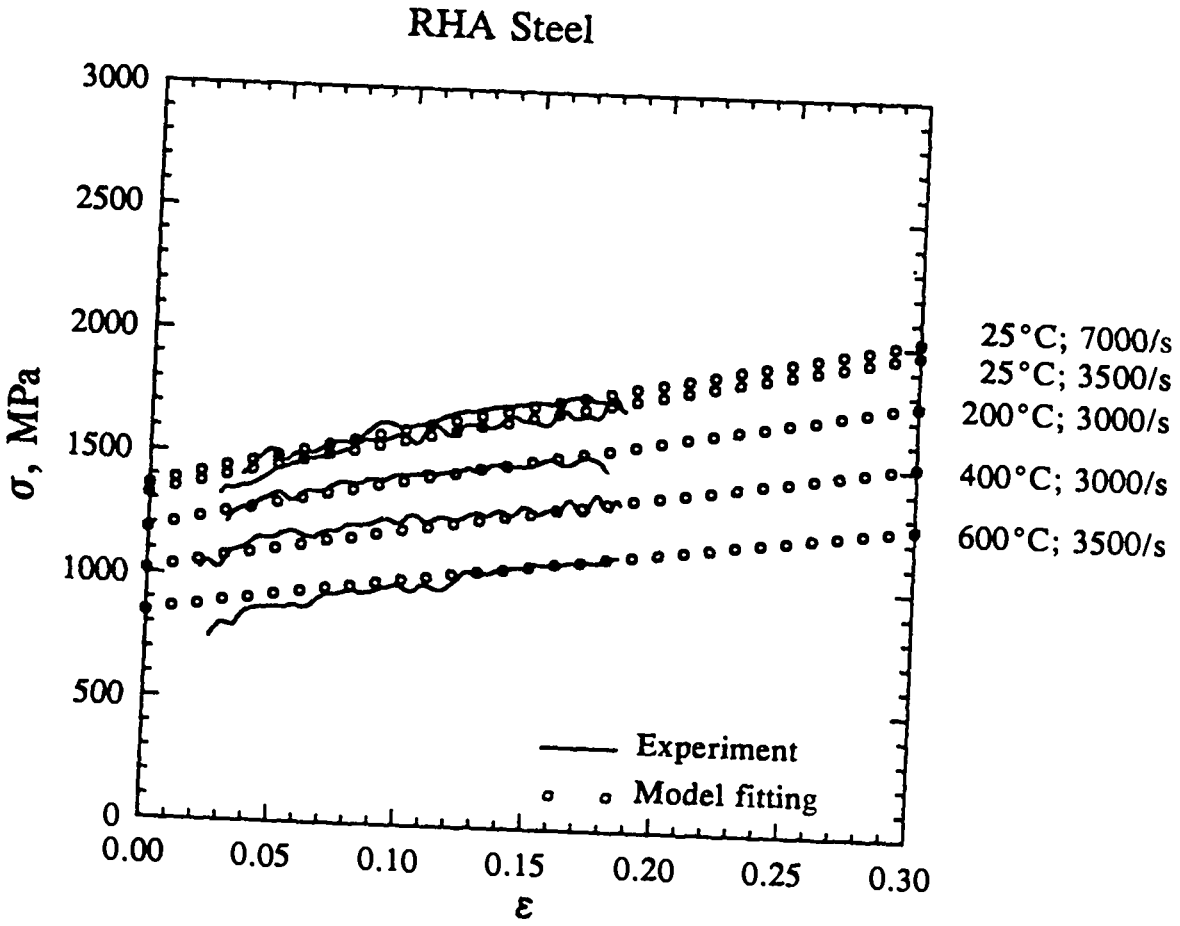

Johnson-Cook Model:

$$\sigma = (A + B\varepsilon^{n})(1 + C\ln\dot{\varepsilon}^{*})(1 - ((T - 298)/(T_m - 298))^{m})$$

$A = 900$ MPa $\quad B = 1305$ MPa $\quad n = 0.9$

$C = 0.0575 \quad m = 1.075 \quad T_m = 1783$ K

Figure 5. Fit of the Al-7039 low and high strain rate data across the temperature range –196°C to 200°C.

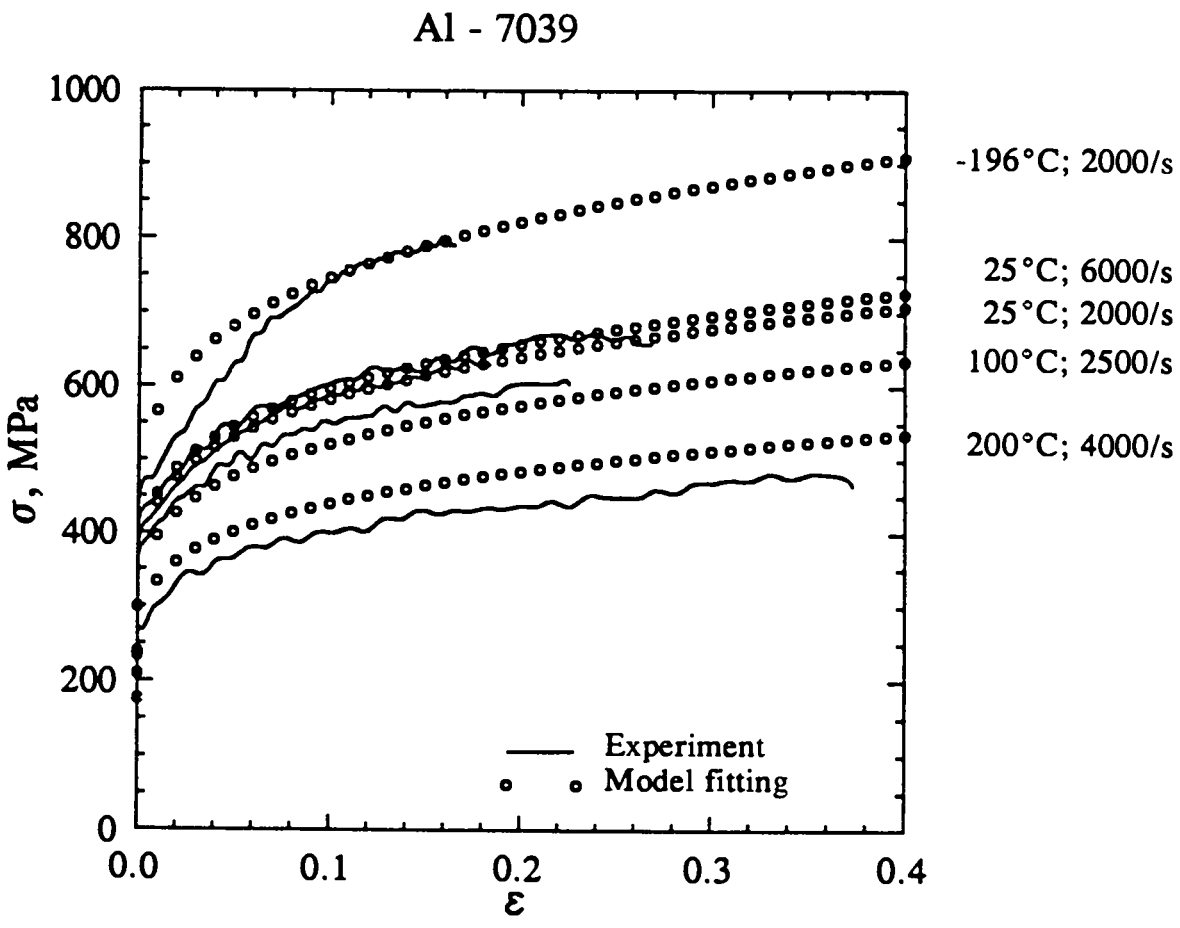

Johnson-Cook Model:

$$\sigma = (A + B\varepsilon^{n})(1 + C\ln\dot{\varepsilon}^{*})(1 - (T/T_{m})^{m})$$

A=260 MPa B=650 MPa n=0.225

C=0.02875 m=1.17 T_m=933 K

Figure 6. Fit of the Al-7039 over the same temperature range (–196°C to 200°C) using only the high strain rate data.

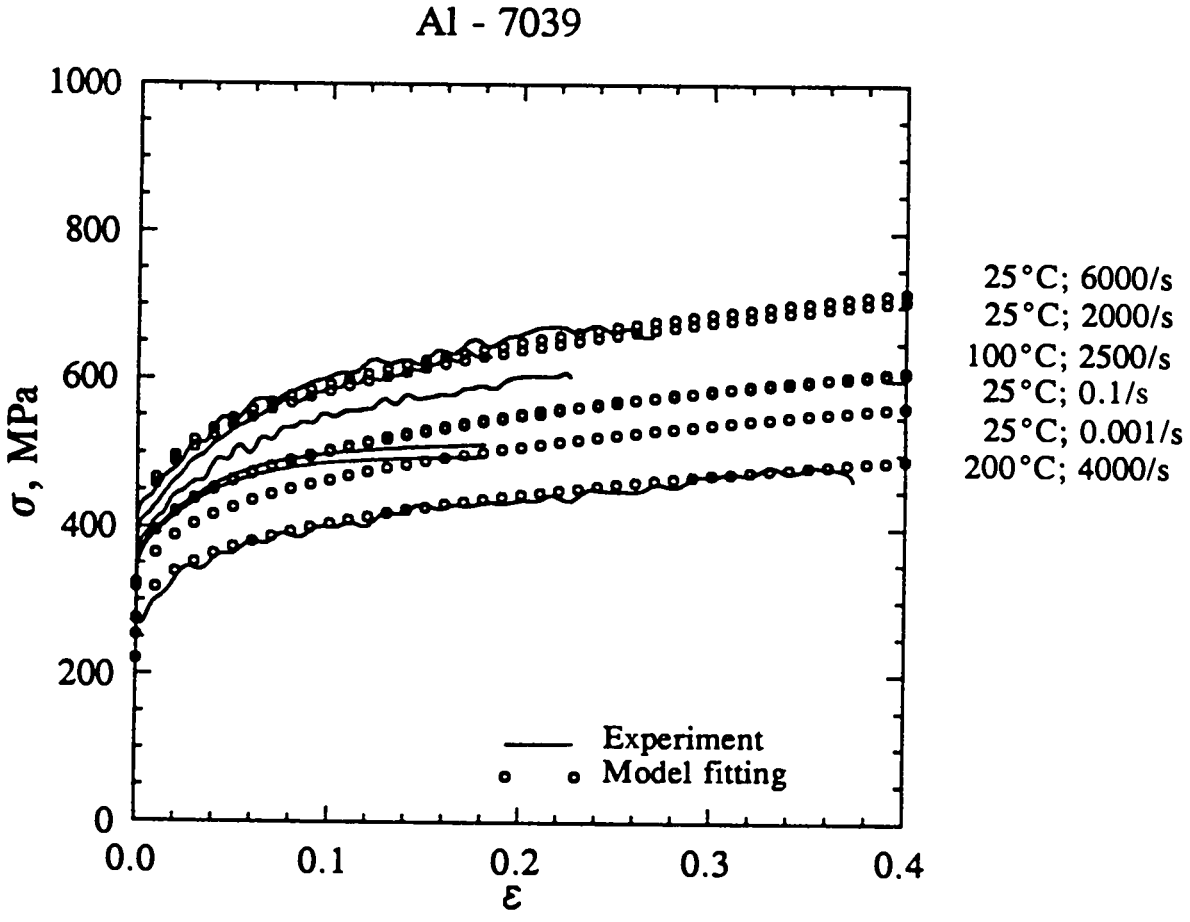

Johnson-Cook Model:

$$\sigma = (A + B\varepsilon^{n})(1 + C\ln\dot{\varepsilon}^{*})(1 - (T/T_m)^{m})$$

A=515 MPa B=810 MPa n=0.2775

C=0.01575 m=0.705 T_m=933 K

Figure 7. Fit of all strain rate data for Al-7039 for RT and above using our homologous T*.

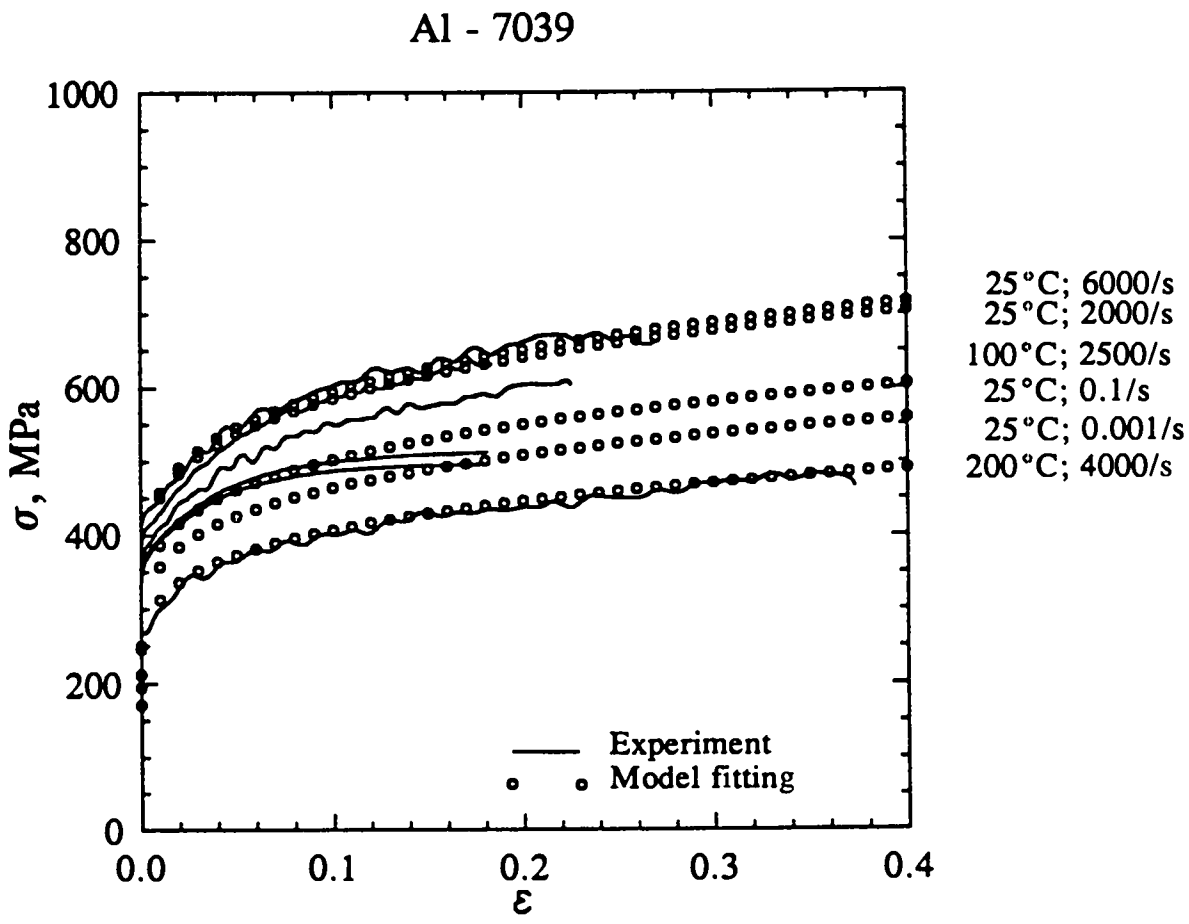

Johnson-Cook Model:

$$\sigma = (A + B\varepsilon^{n})(1 + C\ln\dot{\varepsilon}^{*})(1 - ((T - 298)/(T_m - 298))^{m})$$

A=220 MPa B=500 MPa n=0.22

C=0.016 m=0.905 T_m=933 K

Figure 8. Fit of the same data as Figure 7 but referenced to room temperature using the original Johnson-Cook equation for T*.

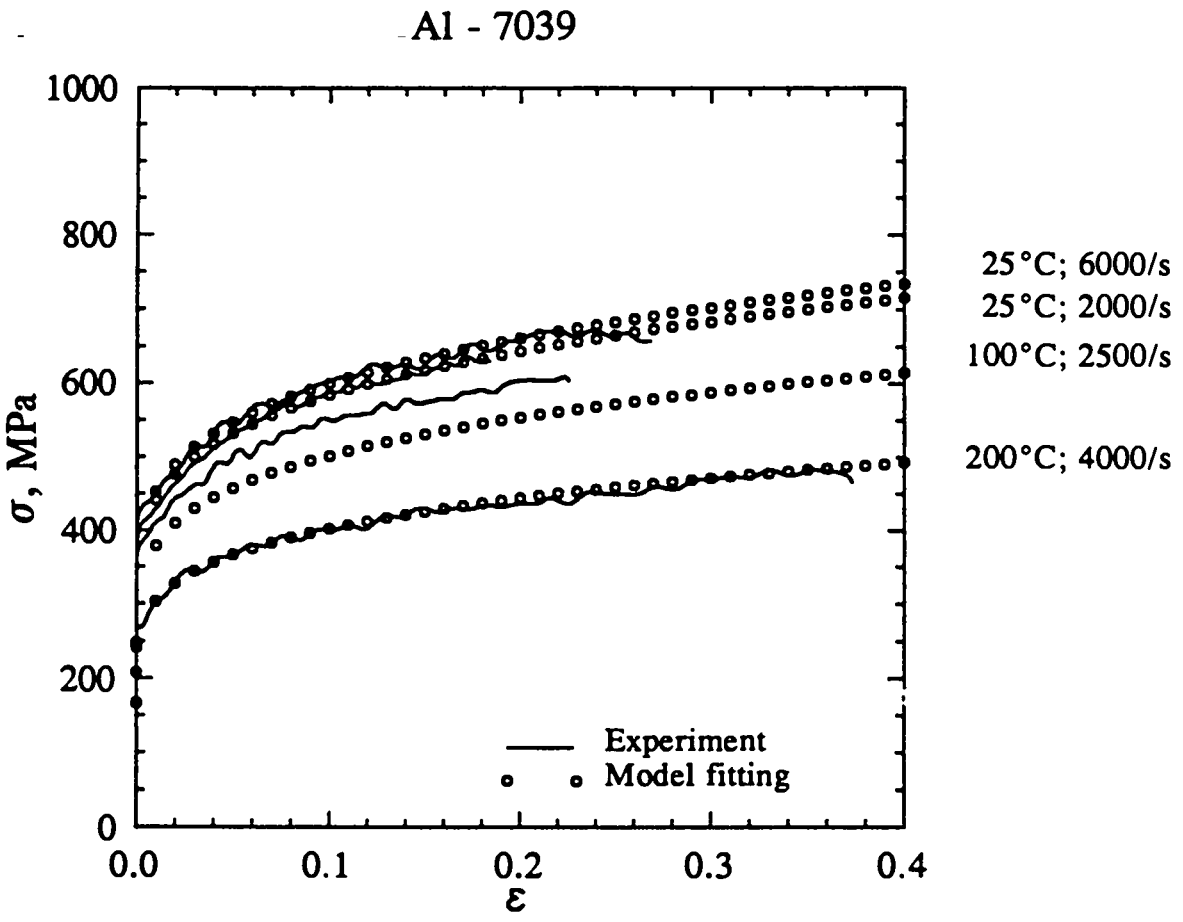

Johnson-Cook Model:

$$\sigma = (A + B\varepsilon^{n})(1 + C\ln\dot{\varepsilon}^{*})(1 - (T/T_{m})^{m})$$

A=390 MPa B=945 MPa n=0.235

C=0.0295 m=0.62 T_m=933 K

Figure 9. Fit of the high rate data only for above room temperature using our homologous T*.

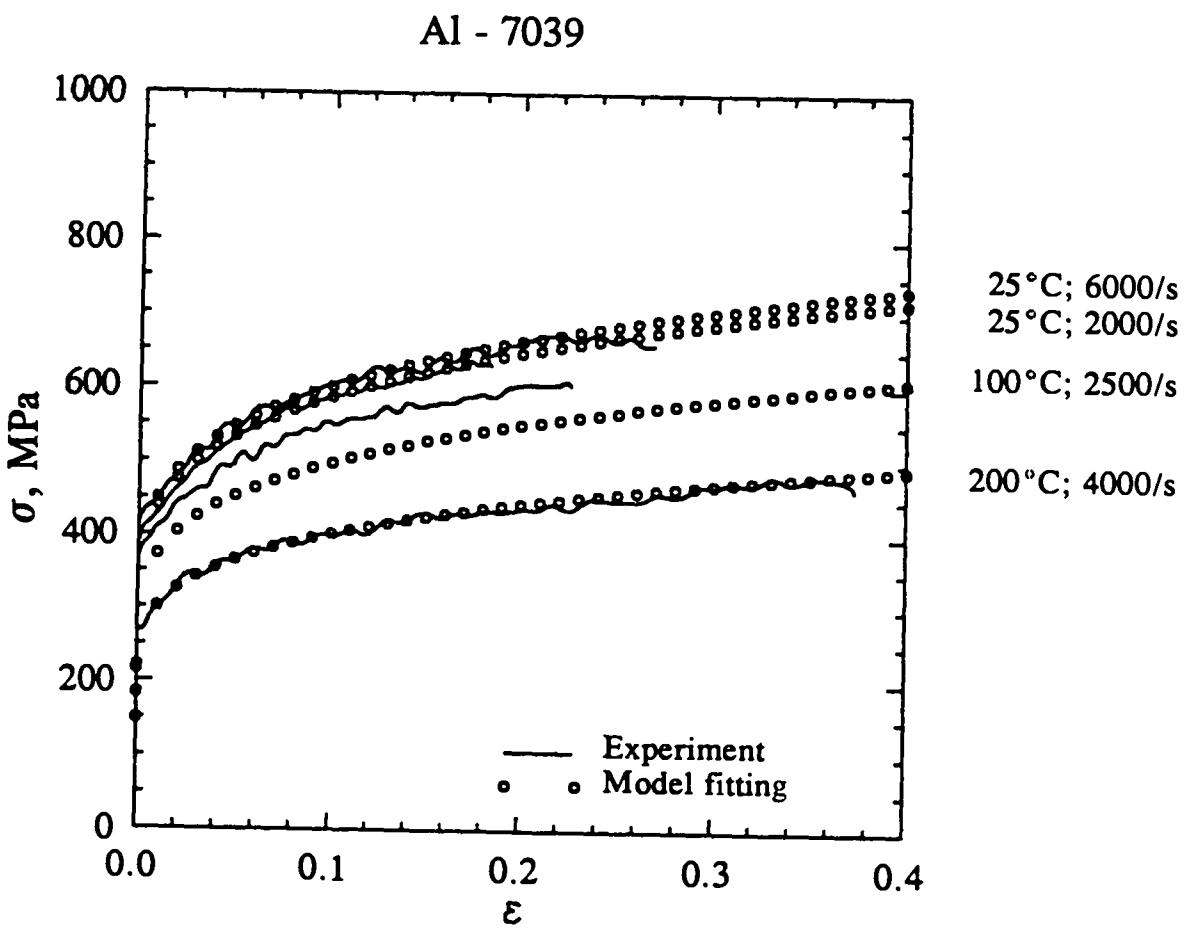

Johnson-Cook Model:

$$\sigma = (A + B\varepsilon^{n})(1 + C\ln\dot{\varepsilon}^{*})(1 - ((T - 298)/(T_m - 298))^{m})$$

$A=180$ MPa $B=510$ MPa $n=0.22$

$C=0.0265$ $m=0.875$ $T_m=933$ K

Figure 10. Fit of the high rate data only for above room temperature using the original Johnson-Cook equation for T*.

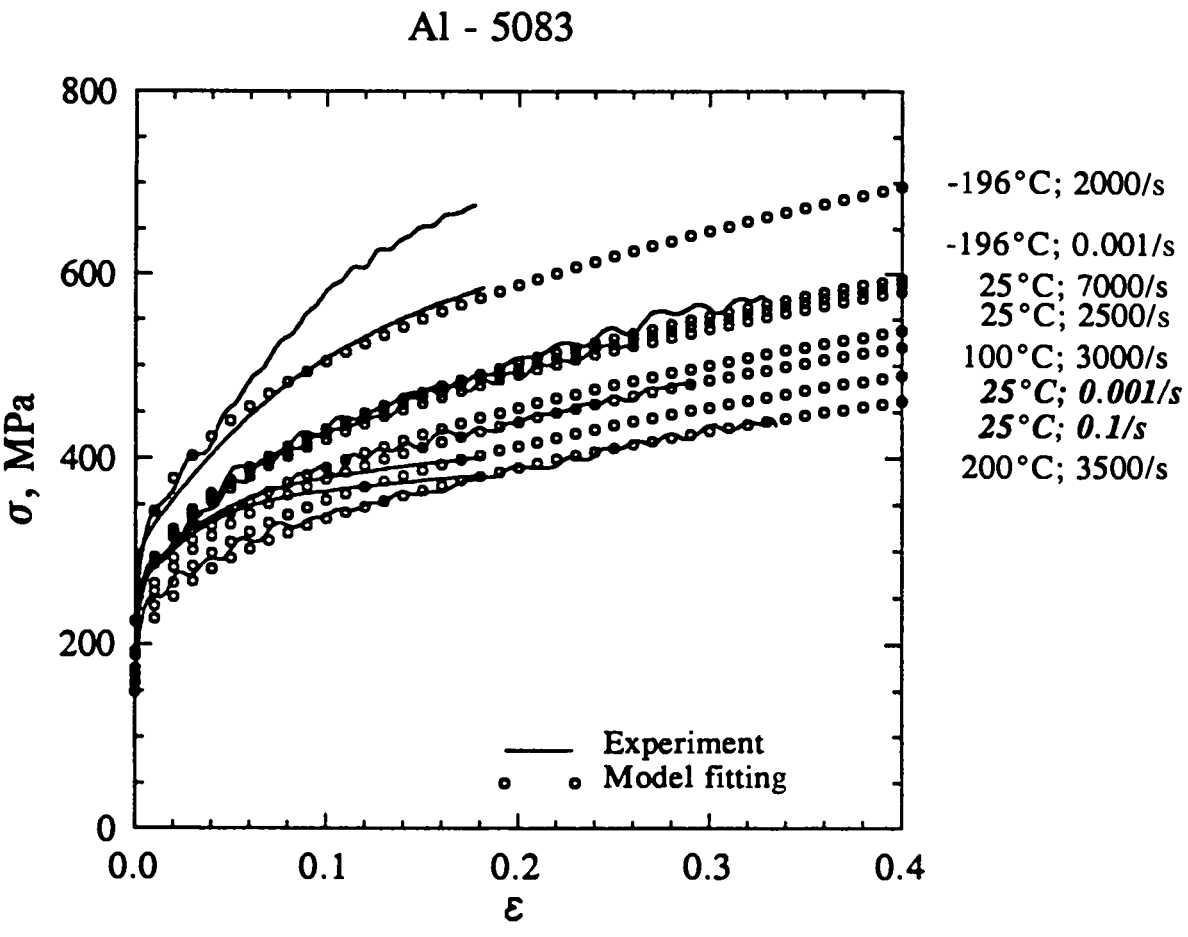

Johnson-Cook Model:

$$\sigma = (A + B\varepsilon^{n})(1 + C\ln\dot{\varepsilon}^{*})(1 - (T/T_{m})^{m})$$

A=210 MPa B=620 MPa n=0.375

C=0.0125 m=1.525 T_m=933 K

Figure 11. Fit of the Al-5083 low and high strain rate data across the temperature range –196°C to 200°C.

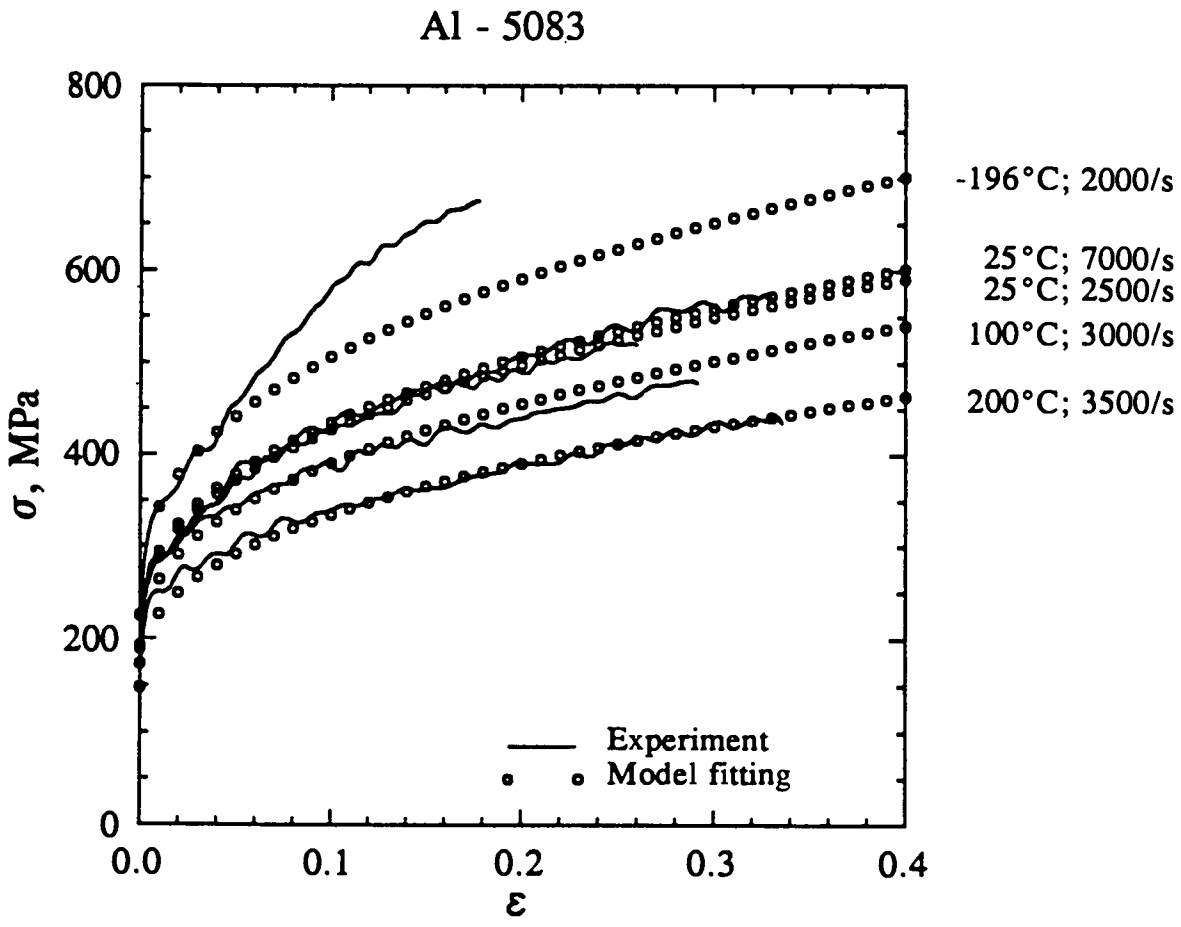

Johnson-Cook Model:

$$\sigma = (A + B\varepsilon^{n})(1 + C\ln\dot{\varepsilon}^{*})(1 - (T/T_{m})^{m})$$

A=200 MPa B=600 MPa n=0.38

C=0.02 m=1.5 T_m=933 K

Figure 12. Fit of Al-5083 over the same temperature range (–196°C to 200°C) using only the high strain rate data.

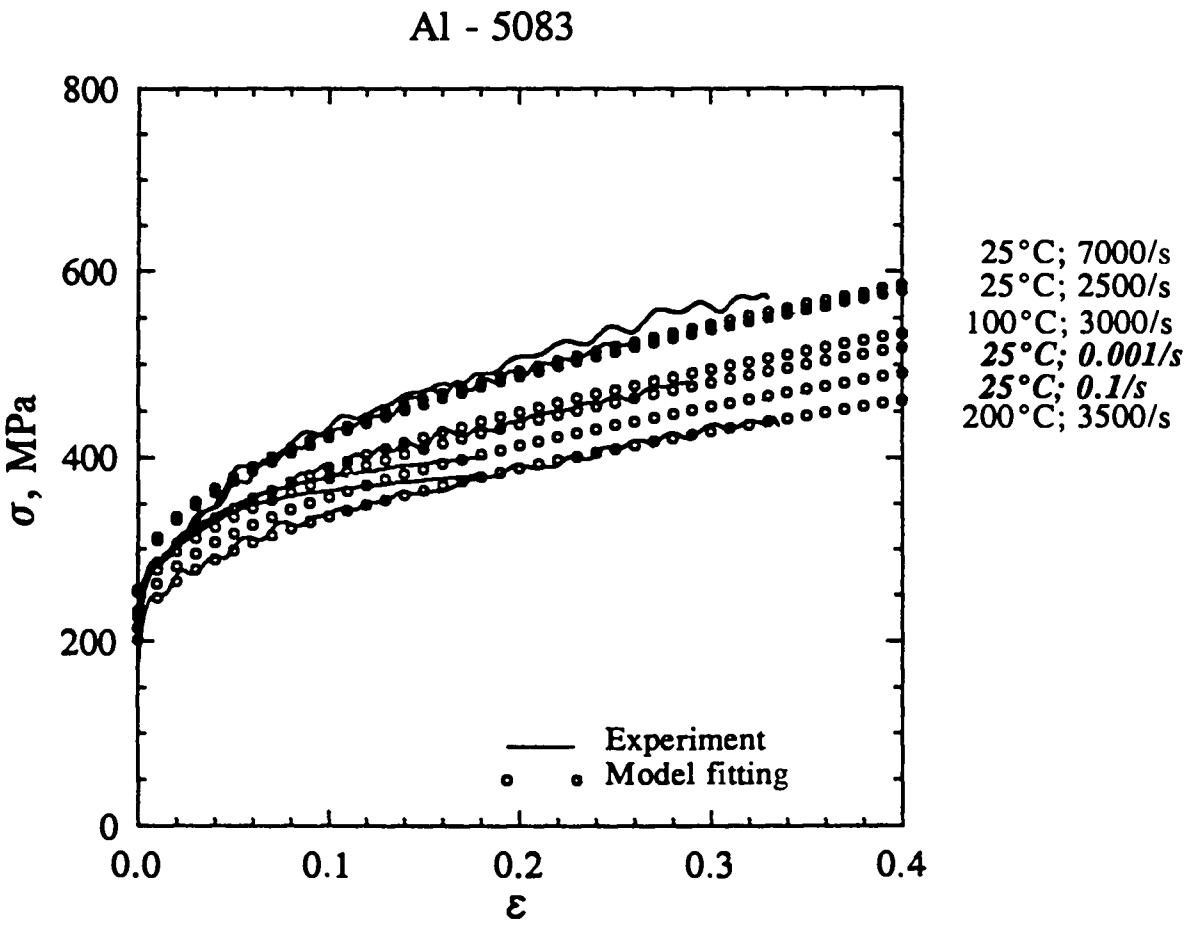

Johnson-Cook Model:

$$\sigma = (A + B\varepsilon^{n})(1 + C\ln\dot{\varepsilon}^{*})(1 - (T/T_{m})^{m})$$

A=275 MPa B=545 MPa n=0.475

C=0.01125 m=1.65 T_m=933 K

Figure 13. Fit of all strain rate data for Al-5083 for RT and above using our homologous T*.

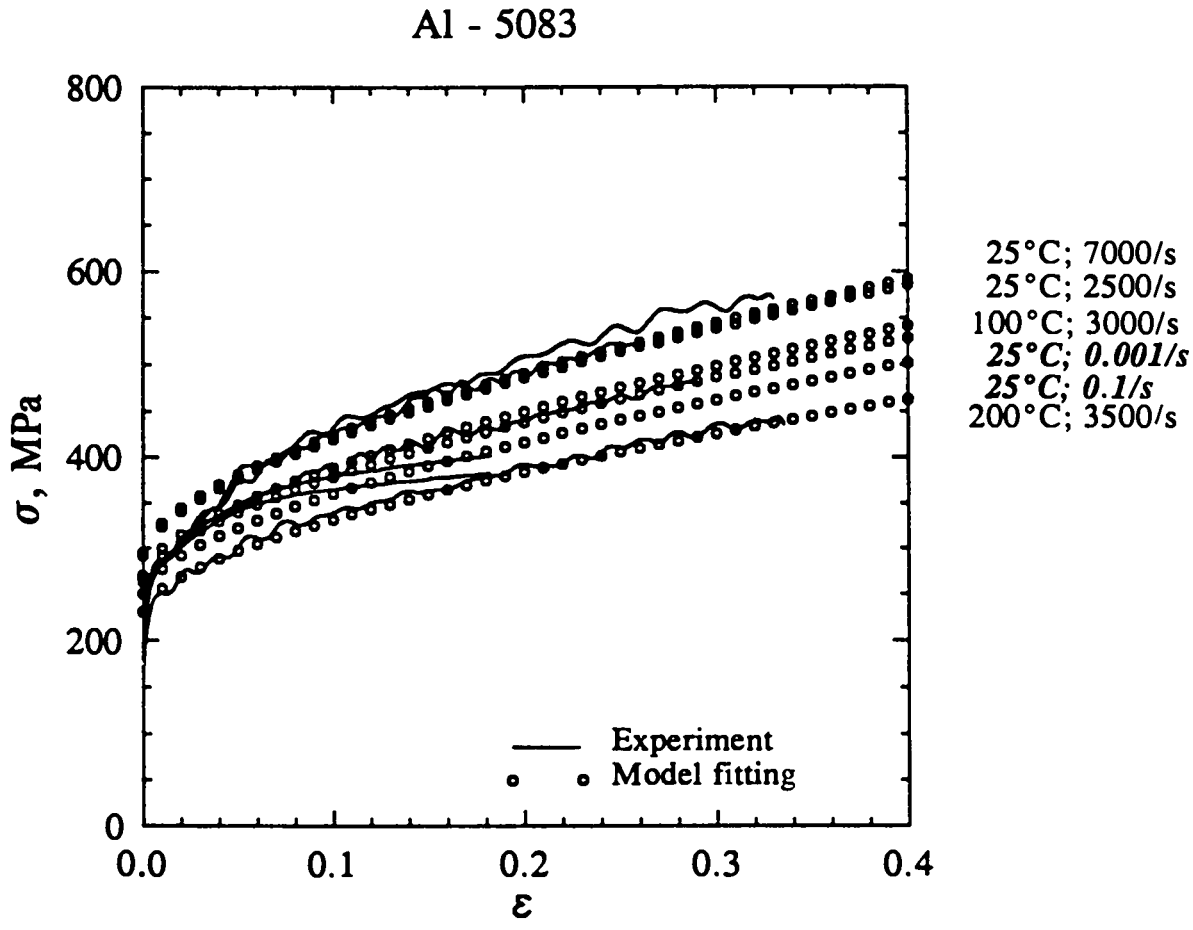

Johnson-Cook Model:

$$\sigma = (A + B\varepsilon^{n})(1 + C\ln\dot{\varepsilon}^{*})(1 - ((T - 298)/(T_m - 298))^{m})$$

A=270 MPa B=470 MPa n=0.6

C=0.0105 m=1.2 T_m=933 K

Figure 14. Fit of the same data as Figure 13 but referenced to room temperature using the original Johnson-Cook equation for T*.

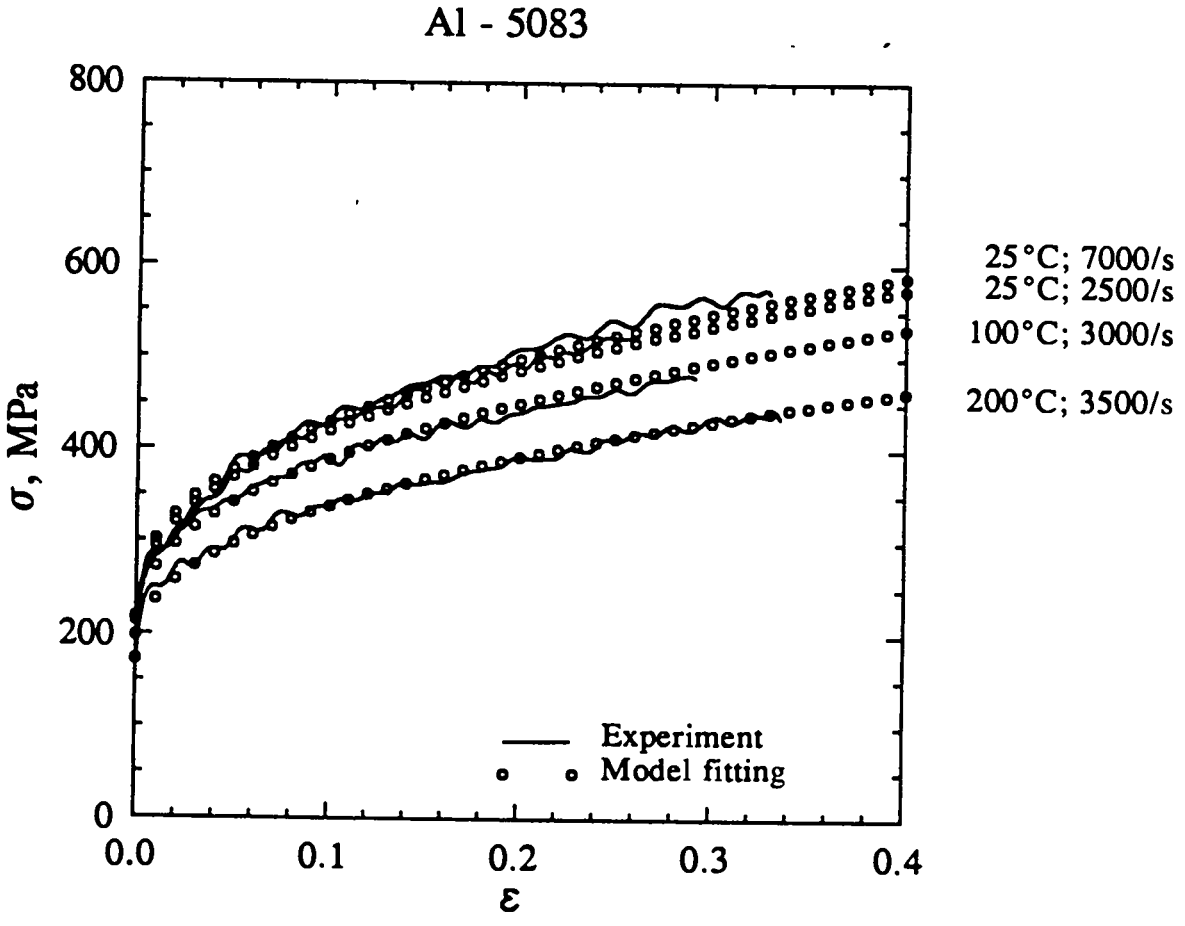

Johnson-Cook Model:

$$\sigma = (A + B\varepsilon^{n})(1 + C\ln\dot{\varepsilon}^{*})(1 - (T/T_{m})^{m})$$

A=205 MPa B=500 MPa n=0.405

C=0.028 m=1.7 T_m=933 K

Figure 15. Fit of the high rate data only for above room temperature using our homologous T*.

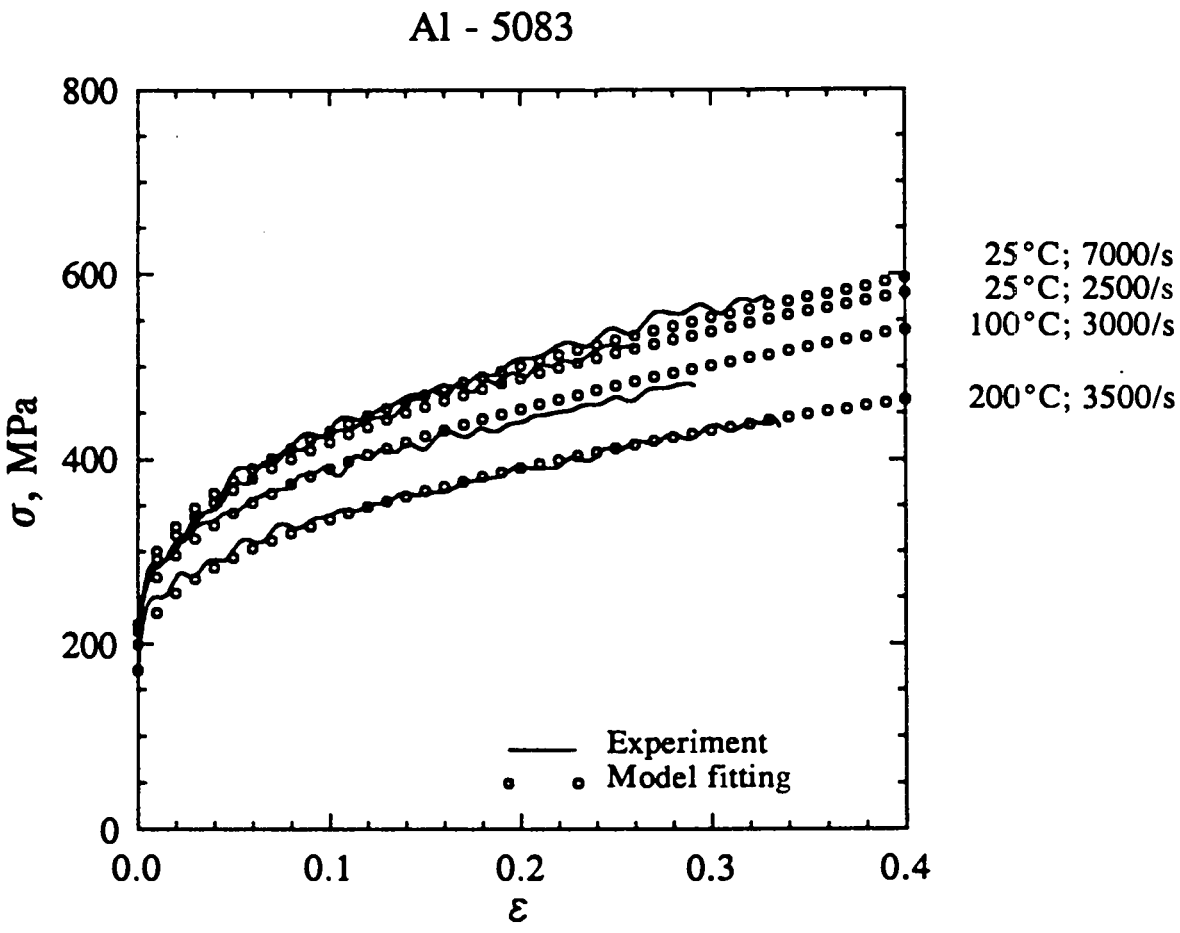

Johnson-Cook Model:

$$\sigma = (A + B\varepsilon^{n})(1 + C\ln\dot{\varepsilon}^{*})(1 - ((T - 298)/(T_m - 298))^{m})$$

A=170 MPa B=425 MPa n=0.42

C=0.0335 m=1.225 T_m=933 K

Figure 16. Fit of the high rate data only for above room temperature using the original Johnson-Cook equation for T*.

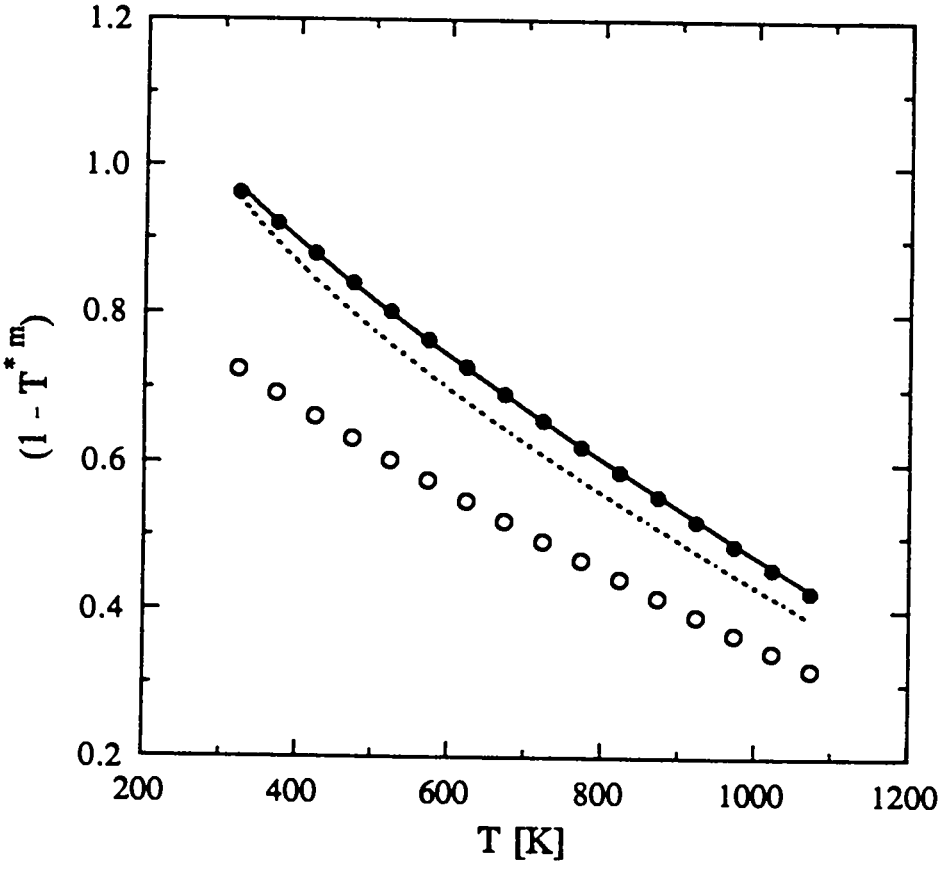

Take 4340 for example; $T_m = 1793$ K

..... $T^* = (T - 298)/(T_m - 298)$; $m = 0.75$

——— $T^* = (T - 298)/(T_m - 298)$; $m = 0.85$

o $T^* = T/T_m$; $m = 0.75$

● $T^* = T/T_m$; $m = 0.75$; times 1.33 to the ordinates of o

Figure 17. Plots of curves of the third term $(1-T^*_m)$ versus temperature.

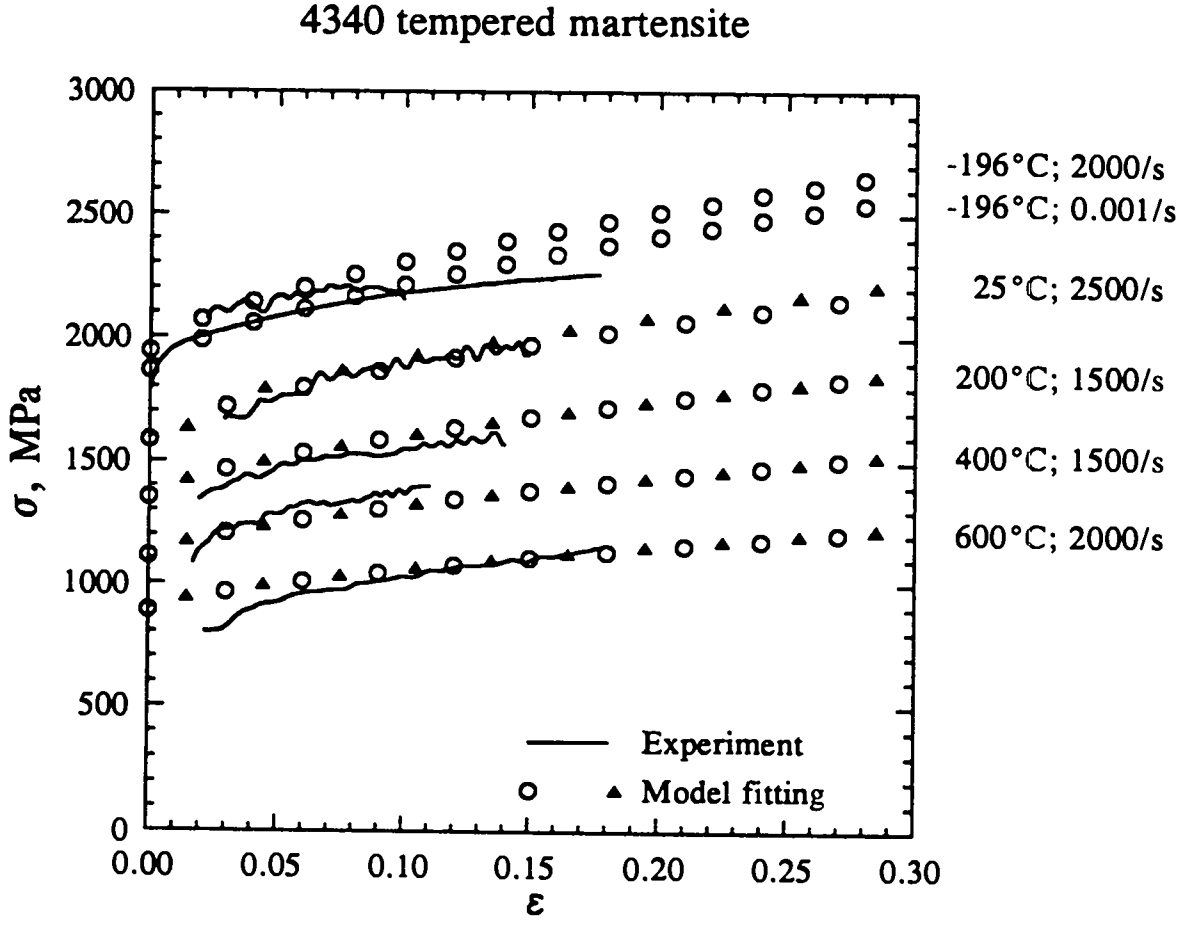

Johnson-Cook Model:

▲ $\sigma = (A + B\varepsilon^{n})(1 + C\ln\dot{\varepsilon}^{*})(1 - ((T - 298)/(T_m - 298))^{m})$

A=1579 MPa B=1316 MPa n=0.65

C=0.0028 m=0.85 T_m=1783 K

o $\sigma = (A + B\varepsilon^{n})(1 + C\ln\dot{\varepsilon}^{*})(1 - (T/T_m)^{m})$

A=2100 MPa B=1750 MPa n=0.65

C=0.0028 m=0.75 T_m=1783 K

Figure 18. Fit of 4340 data using both temperature models with different values of m to preserve the same temperature dependence, a constant ratio of 1.33 between A and B, and n and C the same for both sets of curves. Note the two curves are nearly coincident.

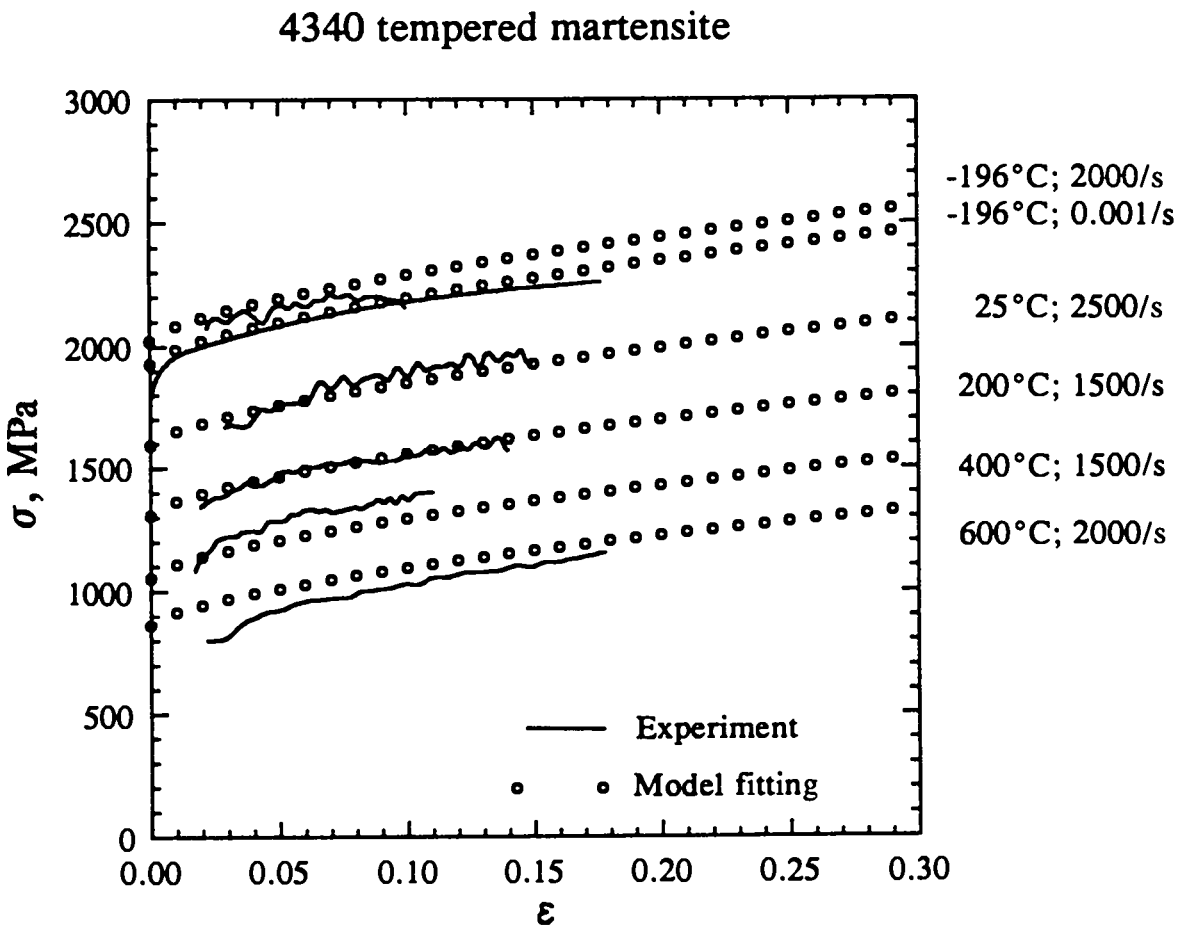

Zerilli-Armstrong Model:

$$\sigma = C_0 + C_1 \exp(-C_3 T + C_4 T \ln\dot{\varepsilon}) + C_5 \varepsilon^n$$

C_0=89.8 MPa C_1=2073.6 MPa C_3=0.0015

C_4=0.0000485 C_5=1029.4 MPa n=0.531

Figure 19. Fit of 4340 data using the Zerilli-Armstrong model.

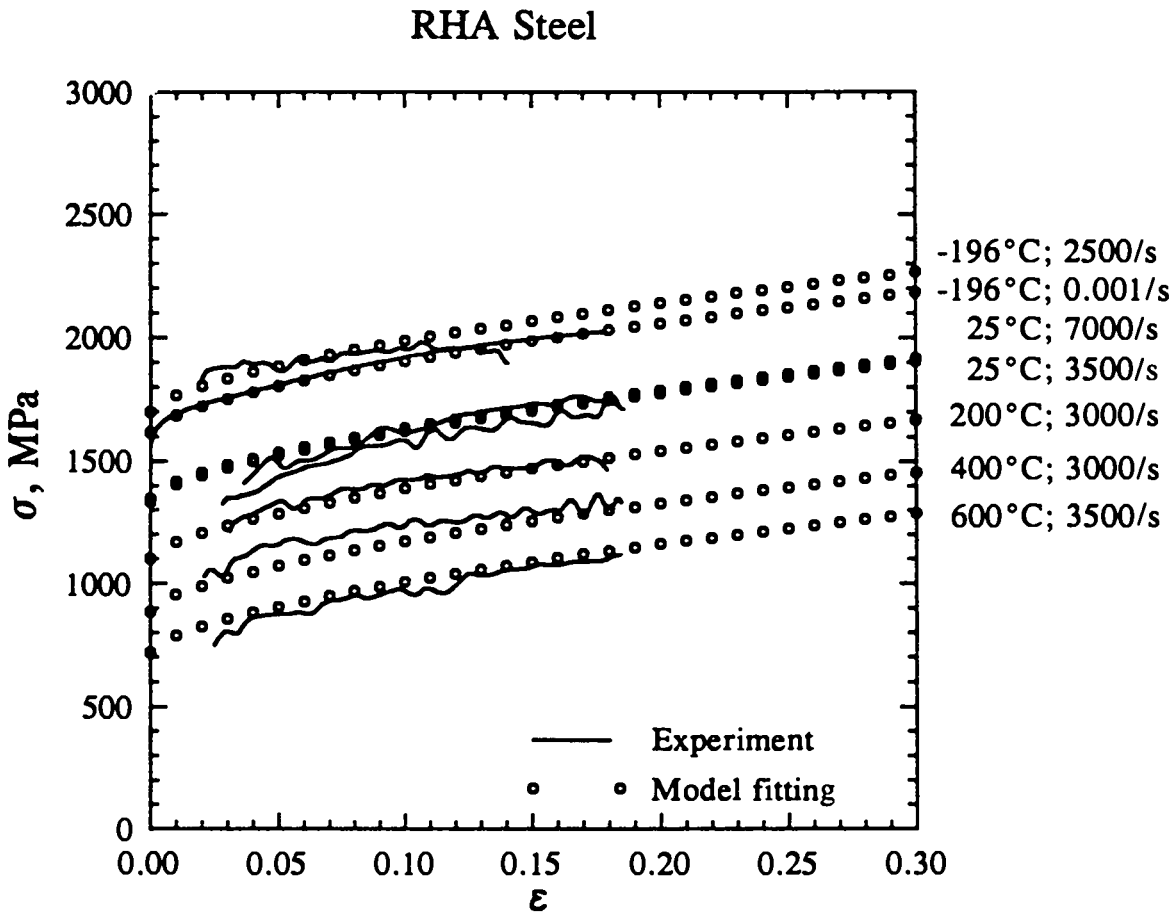

Zerilli-Armstrong Model:

$$\sigma = C_0 + C_1 \exp(-C_3 T + C_4 T \ln\dot{\varepsilon}) + C_5 \varepsilon^n$$

C_0=50 MPa C_1=1800 MPa C_3=0.0015

C_4=0.000045 C_5=1200 MPa n=0.62

Figure 20. Fit of the RHA data using the Zerilli-Armstrong model.

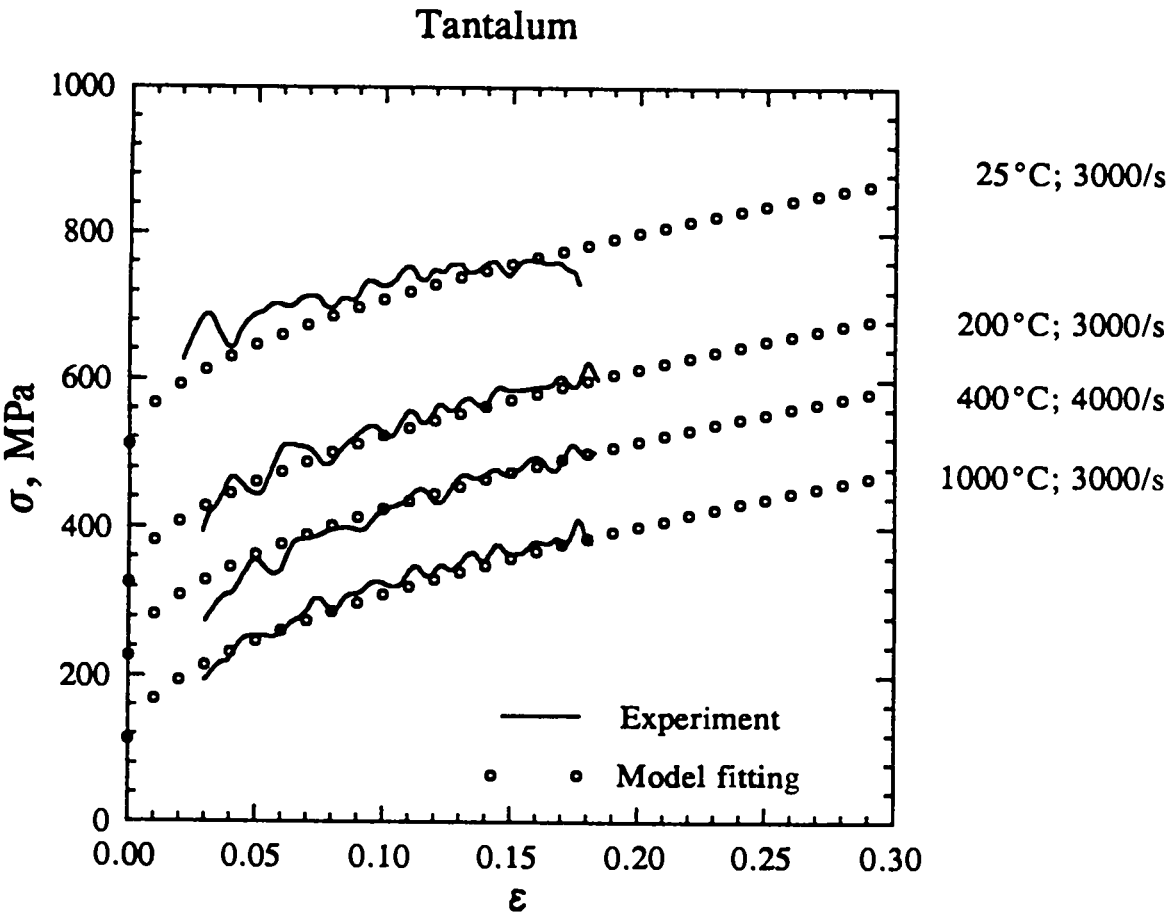

Zerilli-Armstrong Model:

$$\sigma = C_0 + C_1 \exp(-C_3 T + C_4 T \ln\dot{\varepsilon}) + C_5 \varepsilon^n$$

$C_0 = 75$ MPa $C_1 = 1000$ MPa $C_3 = 0.005$

$C_4 = 0.00025$ $C_5 = 700$ MPa $n = 0.5$

Figure 21. Fit of tantalum data using the Zerilli-Armstrong model.

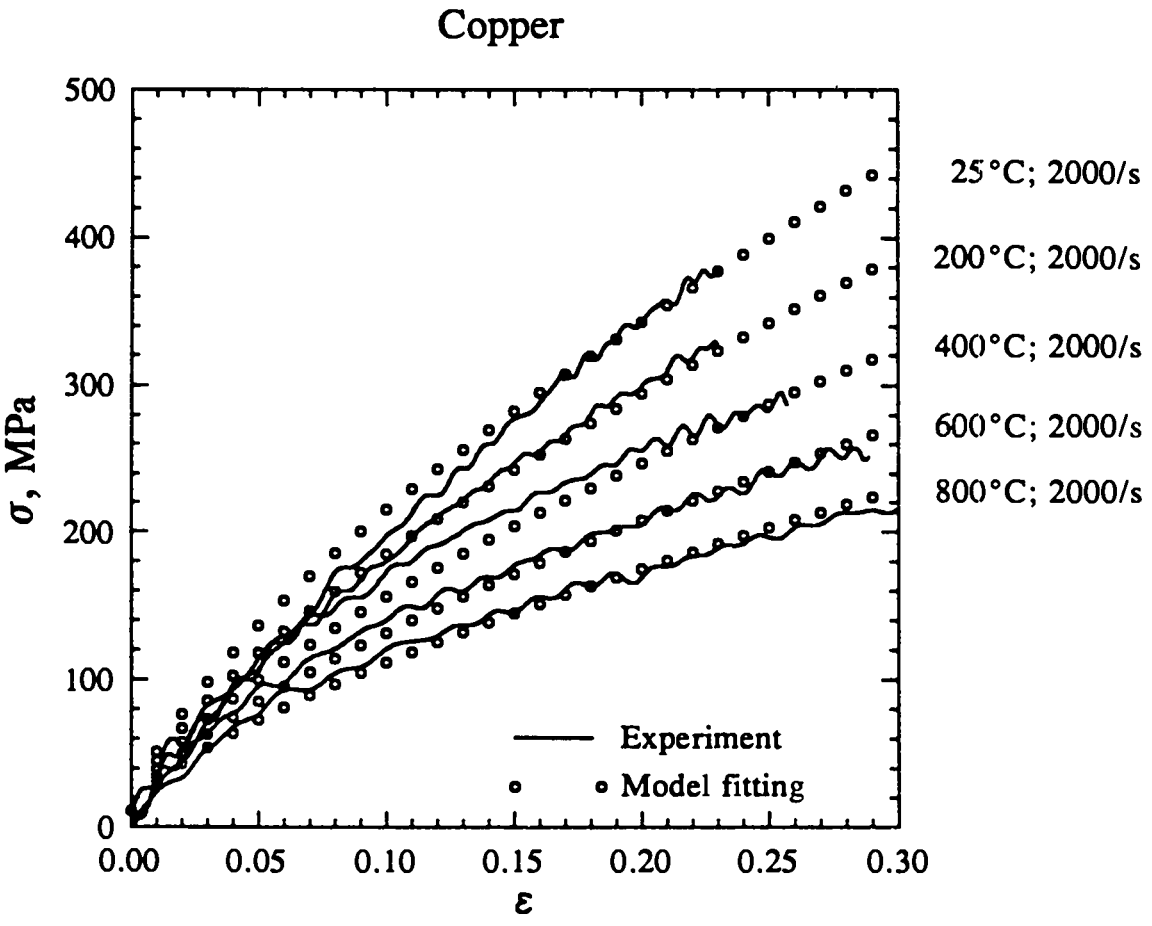

Zerilli-Armstrong Model:

$$\sigma = C_0 + C_2\varepsilon^{n}\exp(-C_3T + C_4T\ln\dot{\varepsilon})$$

C_0=11 MPa C_2=1350 MPa C_3=0.0011

C_4=0.000025 n=0.7025

Figure 22. Fit of copper data using the Zerilli-Armstrong model.

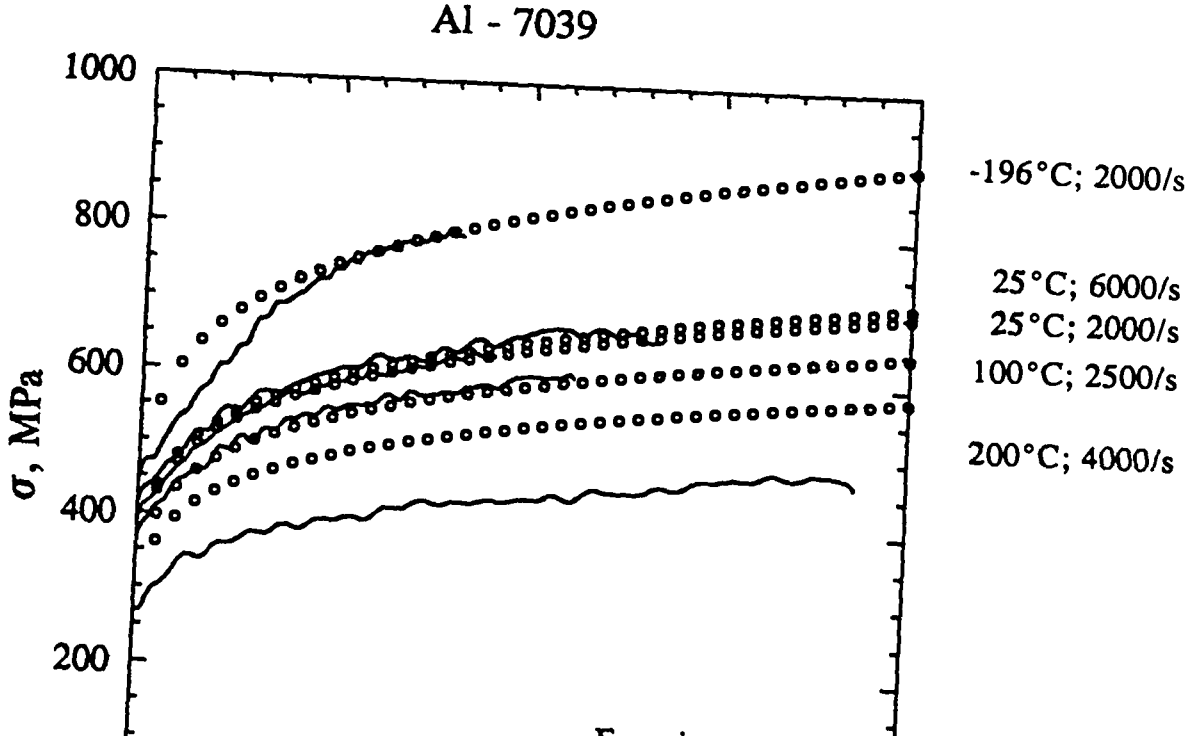

Zerilli-Armstrong Model:

$$\sigma = C_0 + C_2\varepsilon^n \exp(-C_3T + C_4T\ln\dot{\varepsilon})$$

C_0=17 MPa C_2=1090 MPa C_3=0.00155

C_4=0.000052 n=0.135

Figure 23. Fit of Al-7039 data using the Zerilli-Armstrong model.

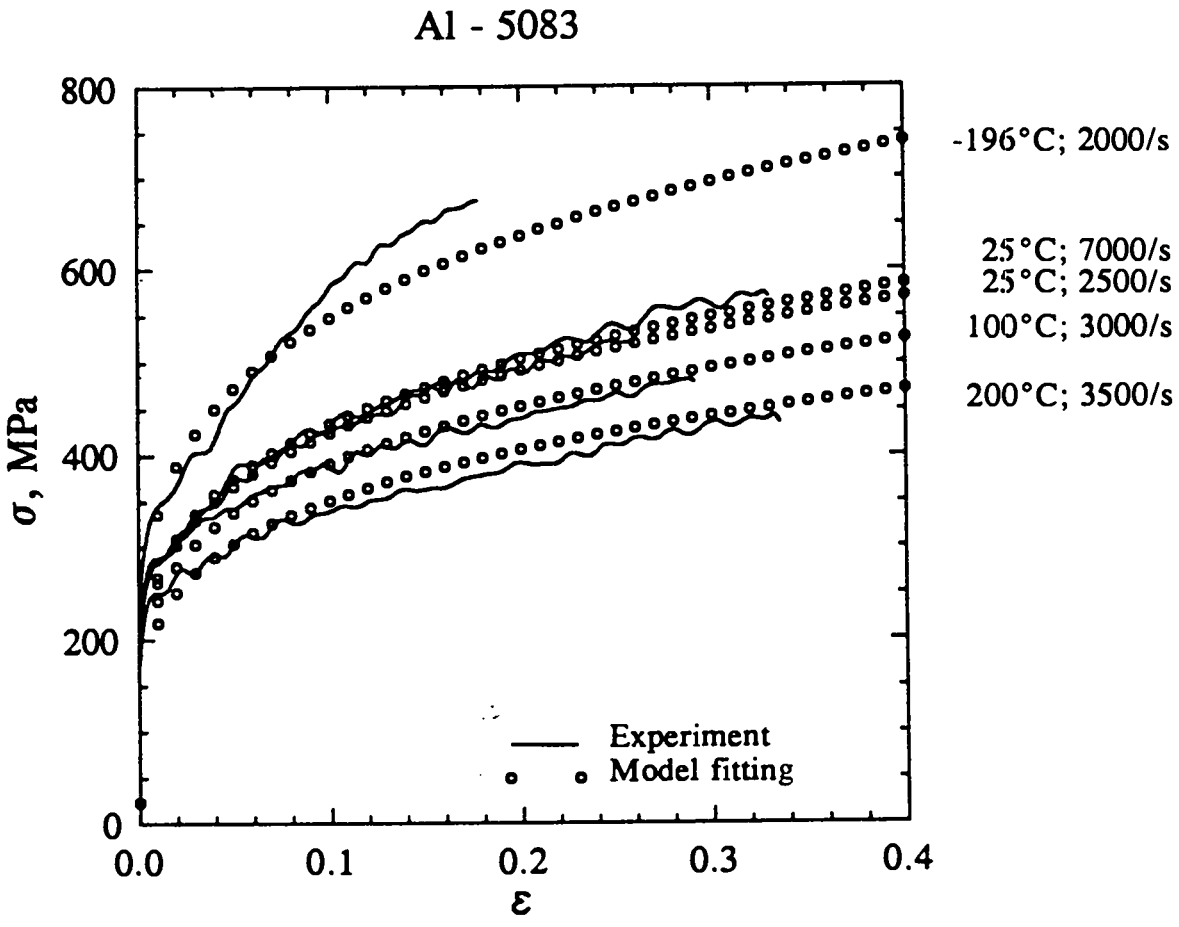

Zerilli-Armstrong Model:

$$\sigma = C_0 + C_2\varepsilon^n \exp(-C_3T + C_4T \ln\dot{\varepsilon})$$

C_0=23 MPa C_2=970 MPa C_3=0.00185

C_4=0.00008 n=0.225

Figure 24. Fit of Al-5083 data using the Zerilli-Armstrong model.

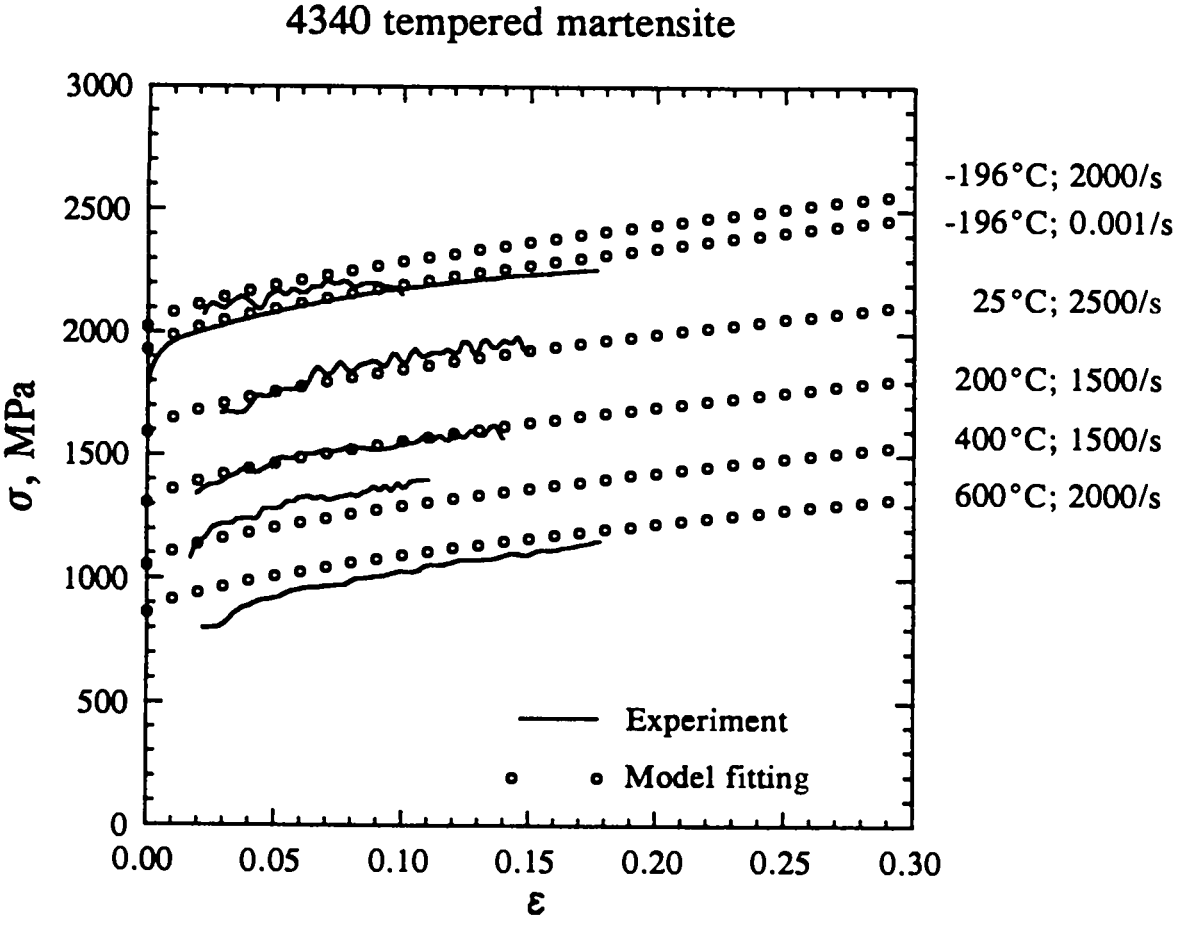

Modified Zerilli-Armstrong Model:

$$\sigma = C_0 + C_1 \exp(-C_3 T + C_4 T \ln\dot{\varepsilon}) + (C_5 \varepsilon^{n} + C_6)\mu(T)/\mu_{293}$$

C_0=100 MPa C_1=2100 MPa C_3=0.0015

C_4=0.000045 C_5=1150 MPa n=0.65 C_6=0 MPa

$$\mu(T)/\mu_{293} = 1.05455 - 0.0001862\ T$$

Figure 25. Fit of 4340 data using the modified Zerilli-Armstrong model.

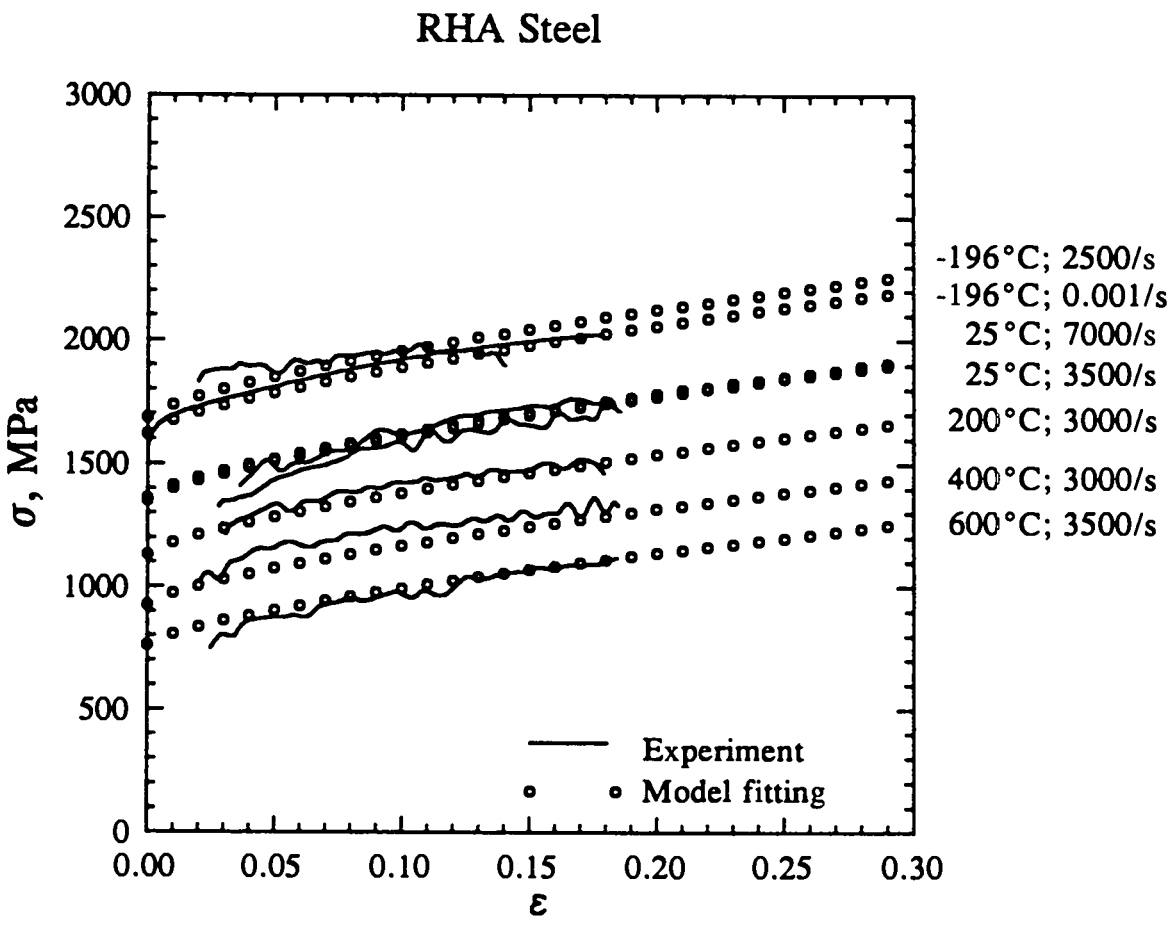

Modified Zerilli-Armstrong Model:

$$\sigma = C_0 + C_1 \exp(-C_3 T + C_4 T \ln\dot{\varepsilon}) + (C_5 \varepsilon^{n} + C_6)\mu(T)/\mu_{293}$$

C_0=20 MPa C_1=1800 MPa C_3=0.0013

C_4=0.000035 C_5=1300 MPa n=0.70 C_6=0

$$\mu(T)/\mu_{293} = 1.05455 - 0.0001862\ T$$

Figure 26. Fit of RHA data using the modified Zerilli-Armstrong model.

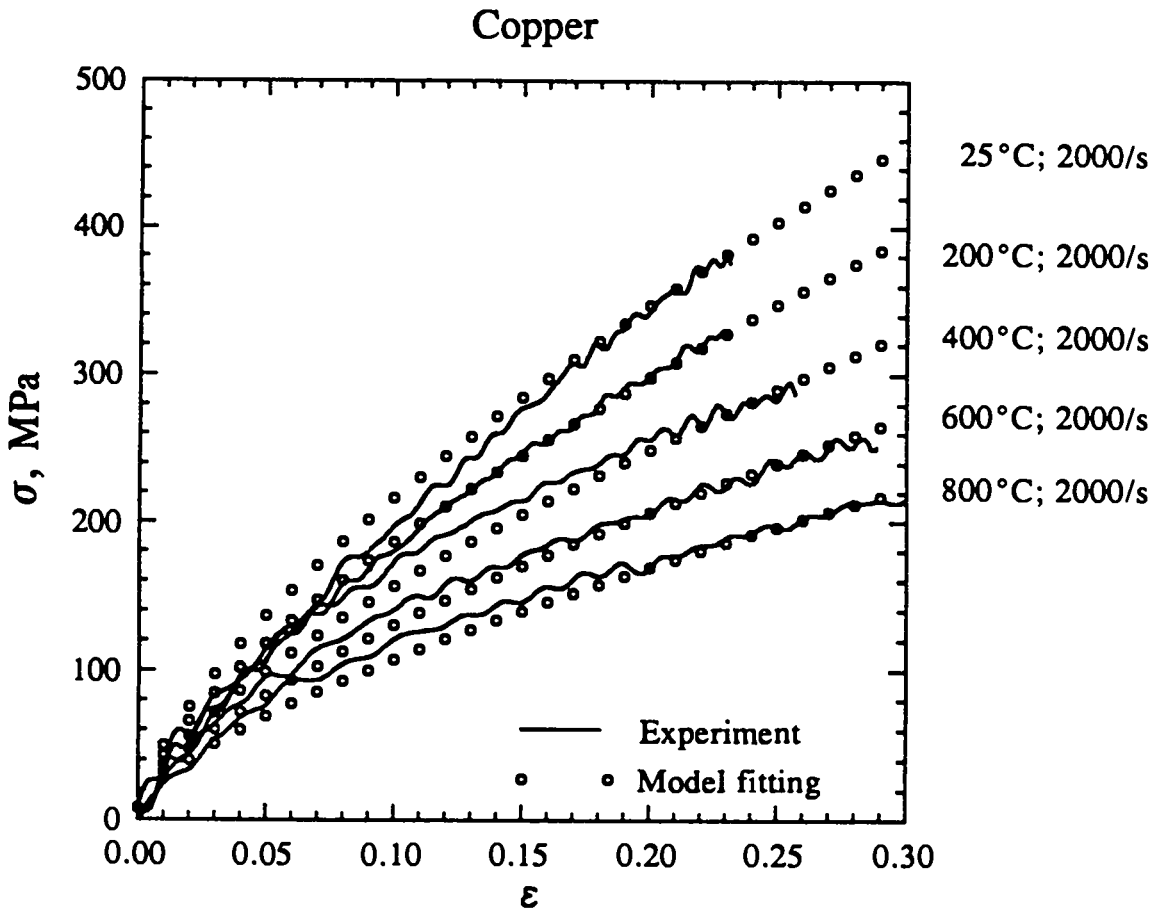

Modified Zerilli-Armstrong Model:

$$\sigma = C_0 + C_2\varepsilon^{n}\exp(-C_3T + C_4T\ln\dot{\varepsilon})\mu(T)/\mu_{293}$$

C_0=8 MPa C_2=1200 MPa C_3=0.0005

C_4=0.000005 n=0.7

$$\mu(T)/\mu_{293} = 1.0842 - 0.08634/(\exp(208/T) - 1)$$

Figure 27. Fit of copper data using the modified Zerilli-Armstrong model.

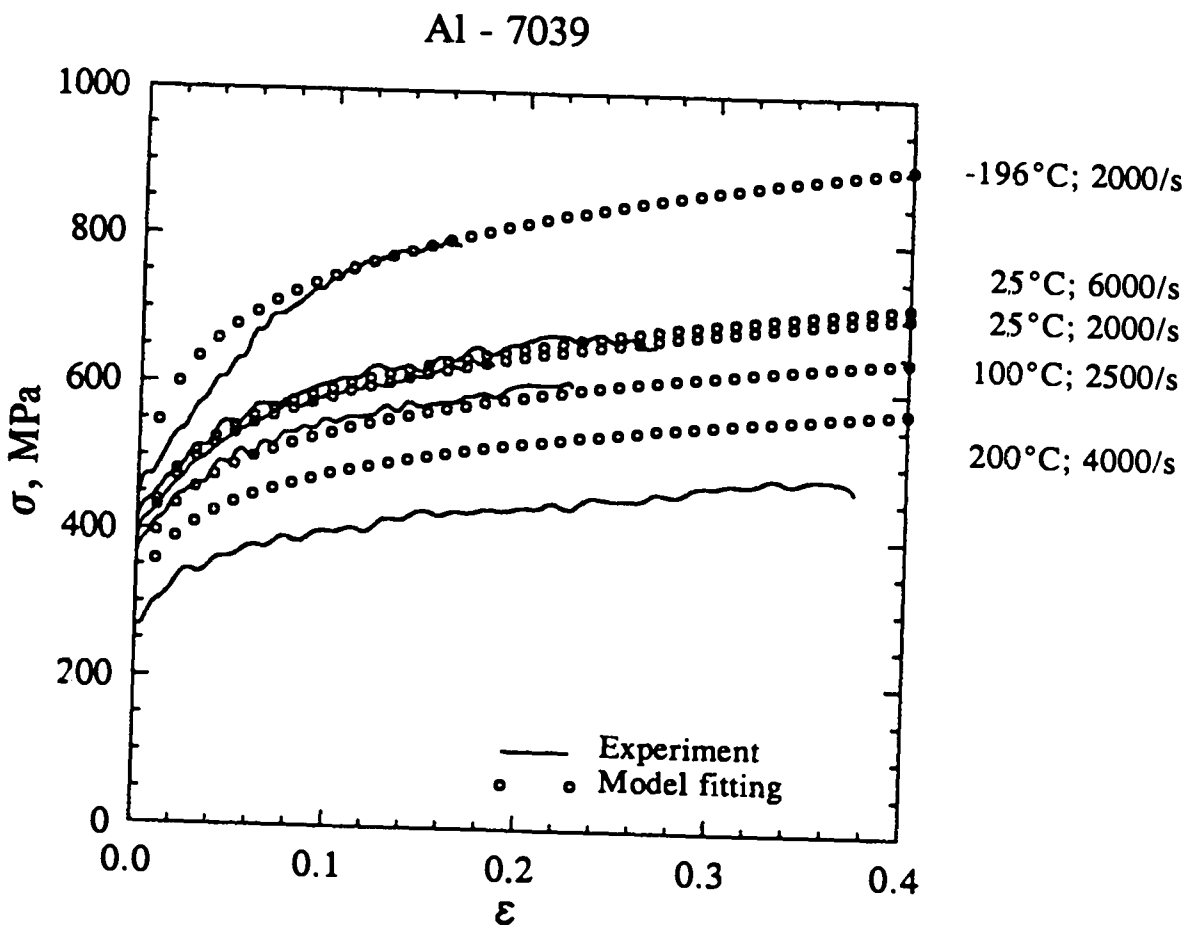

Modified Zerilli-Armstrong Model:

$$\sigma = C_0 + C_2\varepsilon^n \exp(-C_3T + C_4T\ln\dot{\varepsilon})\mu(T)/\mu_{298}$$

C_0=64 MPa C_2=900 MPa C_3=0.00115

C_4=0.0000612 n=0.15

$$\mu(T)/\mu_{298} = 1.13691 - 0.16332/(\exp(234/T) - 1)$$

Figure 28. Fit of Al-7039 data using the modified Zerilli-Armstrong model.

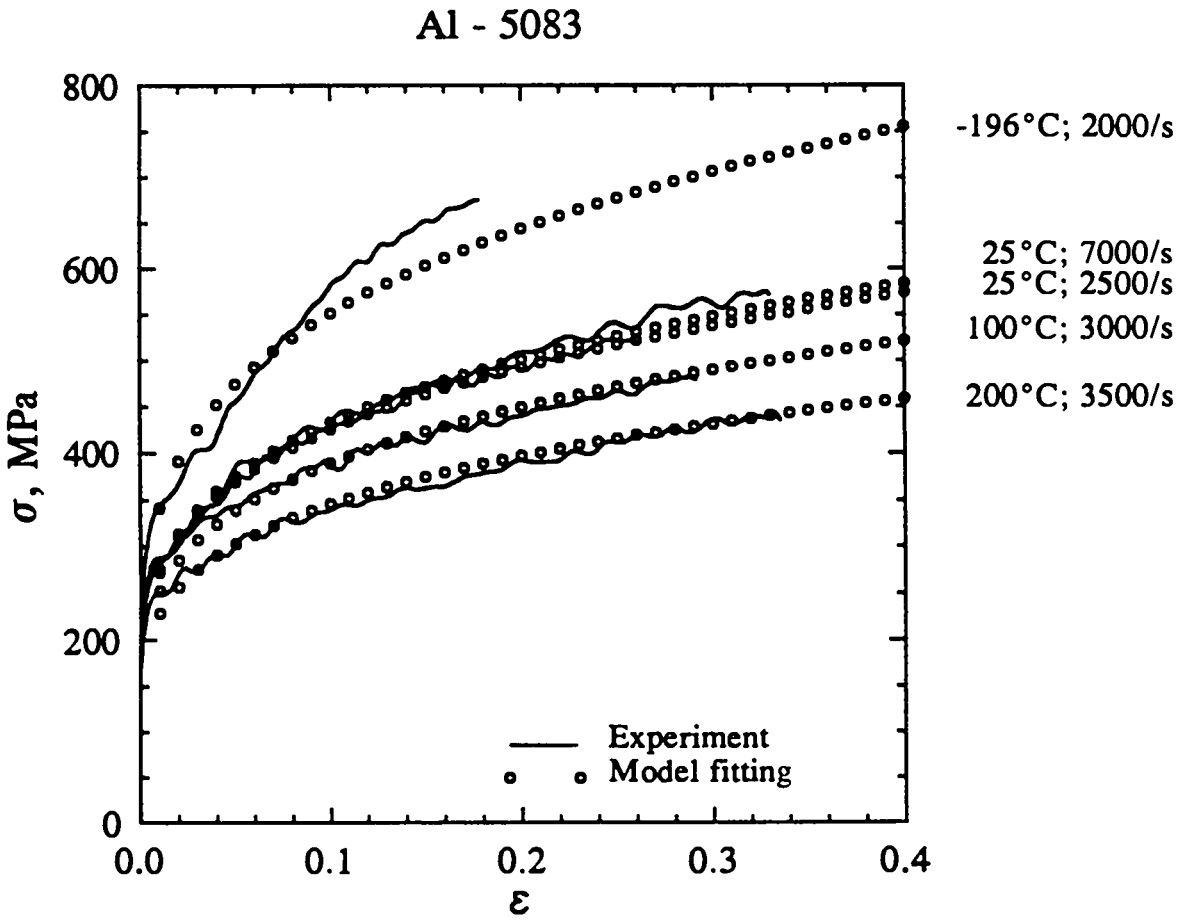

Modified Zerilli-Armstrong Model:

$$\sigma = C_0 + C_2\varepsilon^{n}\exp(-C_3T + C_4T\ln\dot{\varepsilon})\mu(T)/\mu_{298}$$

C_0=91 MPa C_2=805 MPa C_3=0.00145

C_4=0.00007 n=0.265

$$\mu(T)/\mu_{298} = 1.13691 - 0.16332/(\exp(234/T) - 1)$$

Figure 29. Fit of Al-5083 data using the modified Zerilli-Armstrong model.

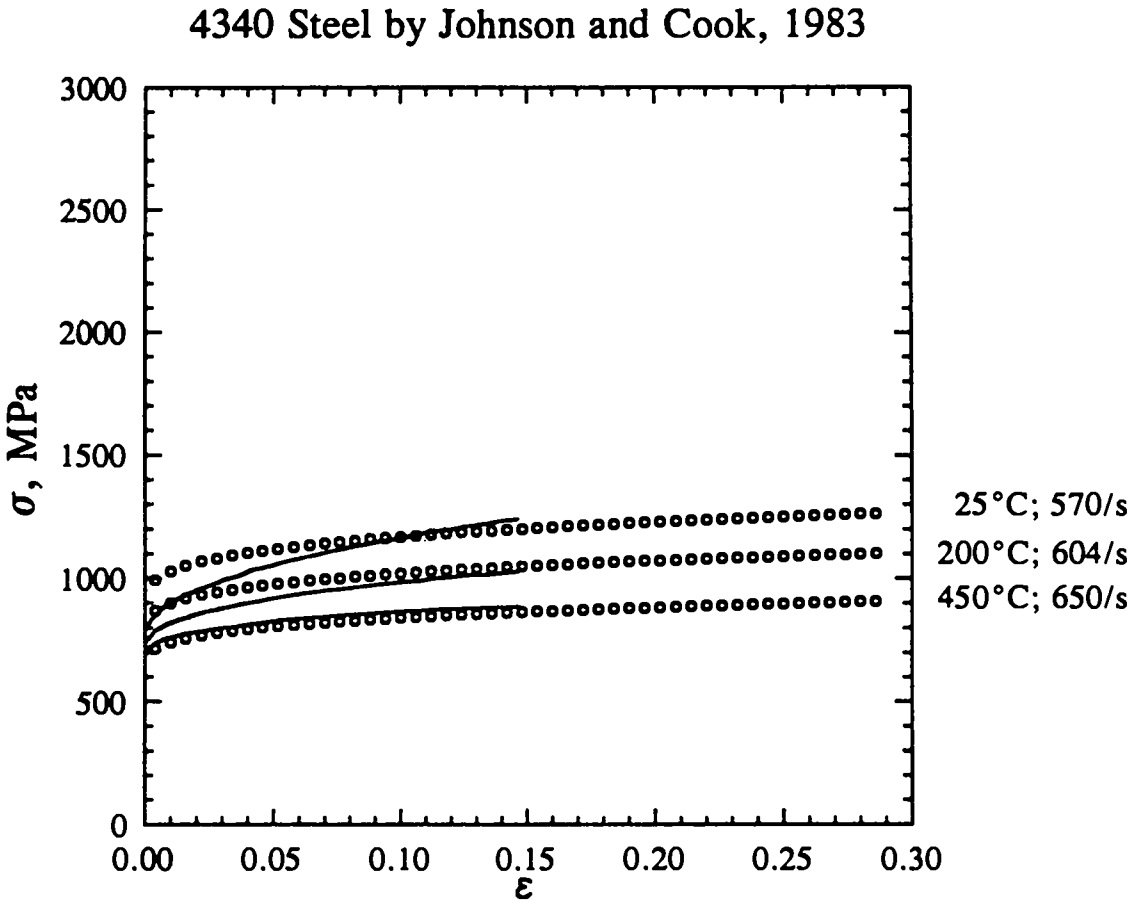

"Proceedings of the Seventh International Symposium on Ballistics",
The Hague, The Netherland, 1983, p.541, Figure 1.

Johnson-Cook Model:

$$\sigma = (A + B\varepsilon^{n})(1 + C\ln\dot{\varepsilon}^{*})(1 - ((T - T_{ROOM})/(T_{MELT} - T_{ROOM}))^{m})$$

$A = 792$ MPa $\quad B = 510$ MPa $\quad n = 0.26$

$C = 0.014 \quad m = 1.03 \quad T_m = 1783$ K

Figure 30. Johnson-Cook fit to 4340 data from 1983. Note the curve only fits the 450°C and 650/s data.

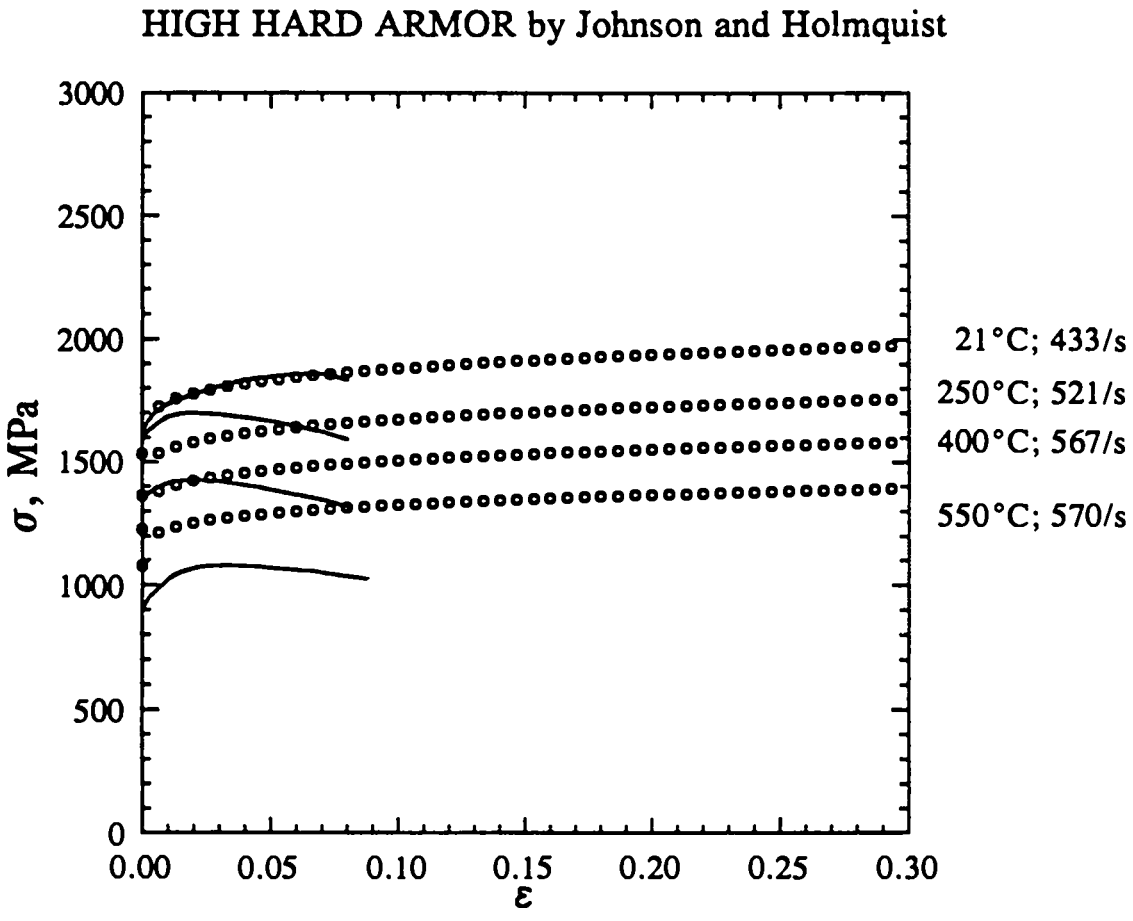

Johnson-Cook Model:

$$\sigma = (A + B\varepsilon^{n})(1 + C\ln\dot{\varepsilon}^{*})(1 - ((T - T_{ROOM})/(T_{MELT} - T_{ROOM}))^{m})$$

A=1504 MPa B=569 MPa n=0.22

C=0.003 m=1.17 T_m=1783 K

Figure 31. Johnson-Cook fit to RHA data from 1983. Curve fits only the room temperature data well.

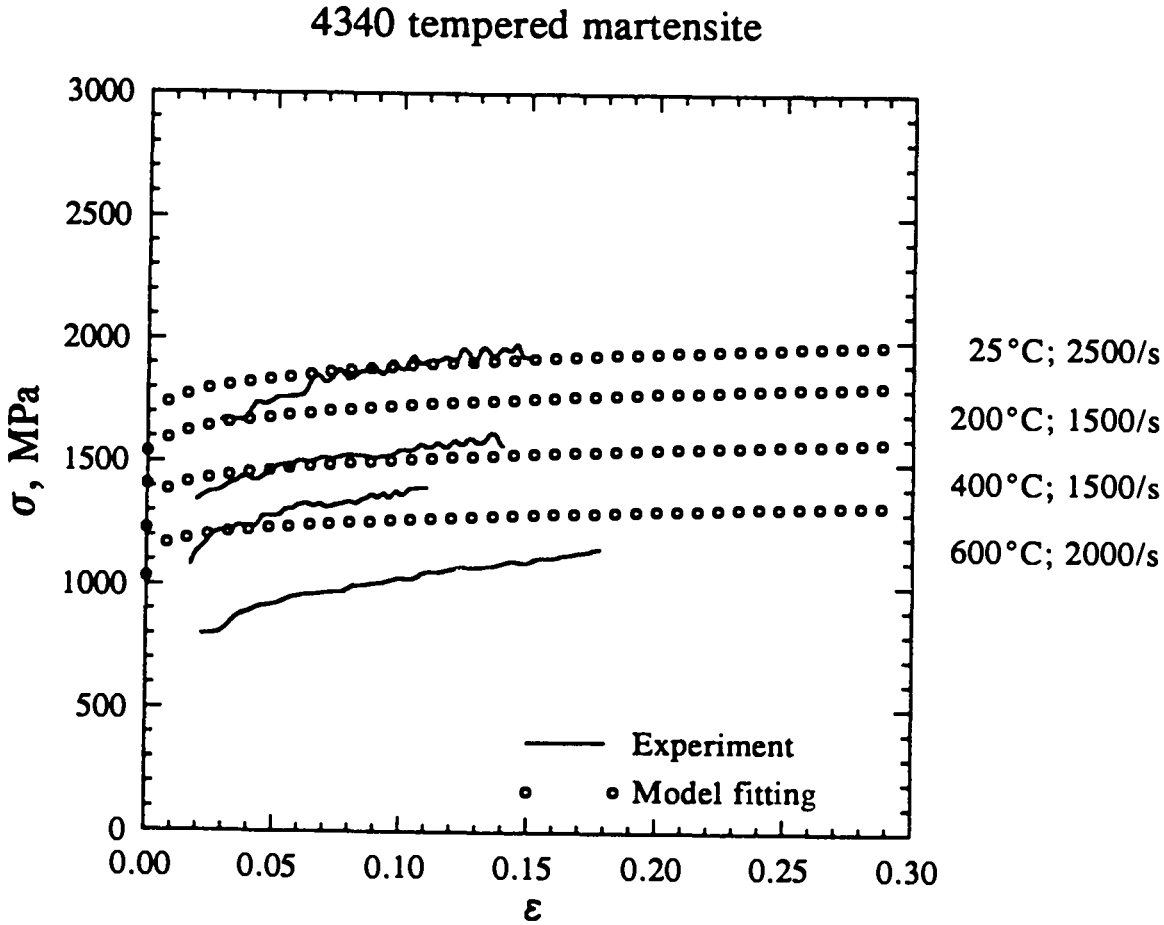

Johnson-Cook Model:

$$\sigma = (A + B\varepsilon^{n})(1 + C\ln\dot{\varepsilon}^{*})(1 - ((T - T_{ROOM})/(T_{MELT} - T_{ROOM}))^{m})$$

Using constants derived by Johnson & Holmquist for

their High Hard Armor :

A=1504 MPa B=569 MPa n=0.22

C=0.003 m=1.17 T_m=1783 K

Figure 32. The set of constants (derived from Figure 31) fits our room temperature data at high strain rates. Our 4340 steel data was obtained on steel reheated, homogenized, quenched, and tempered by Los Alamos.

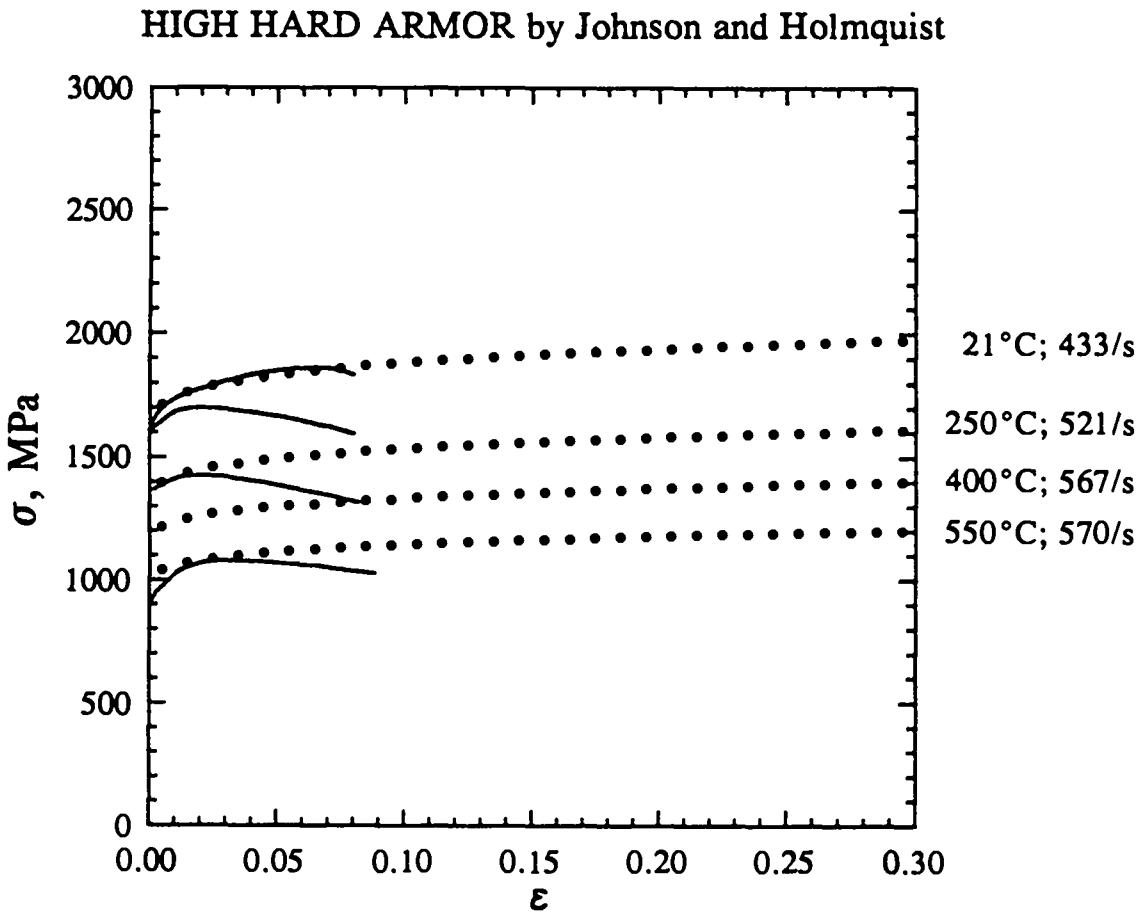

Johnson-Cook Model:

$$\sigma = (A + B\varepsilon^{n})(1 + C\ln\dot{\varepsilon}^{*})(1 - ((T - T_{ROOM})/(T_{MELT} - T_{ROOM}))^{m})$$

A=1504 MPa B=569 MPa n=0.22

C=0.003 ***m=0.90*** T_m=1783 K

Figure 33. Data from Figure 31 fit by changing m from 1.17 to 0.90.

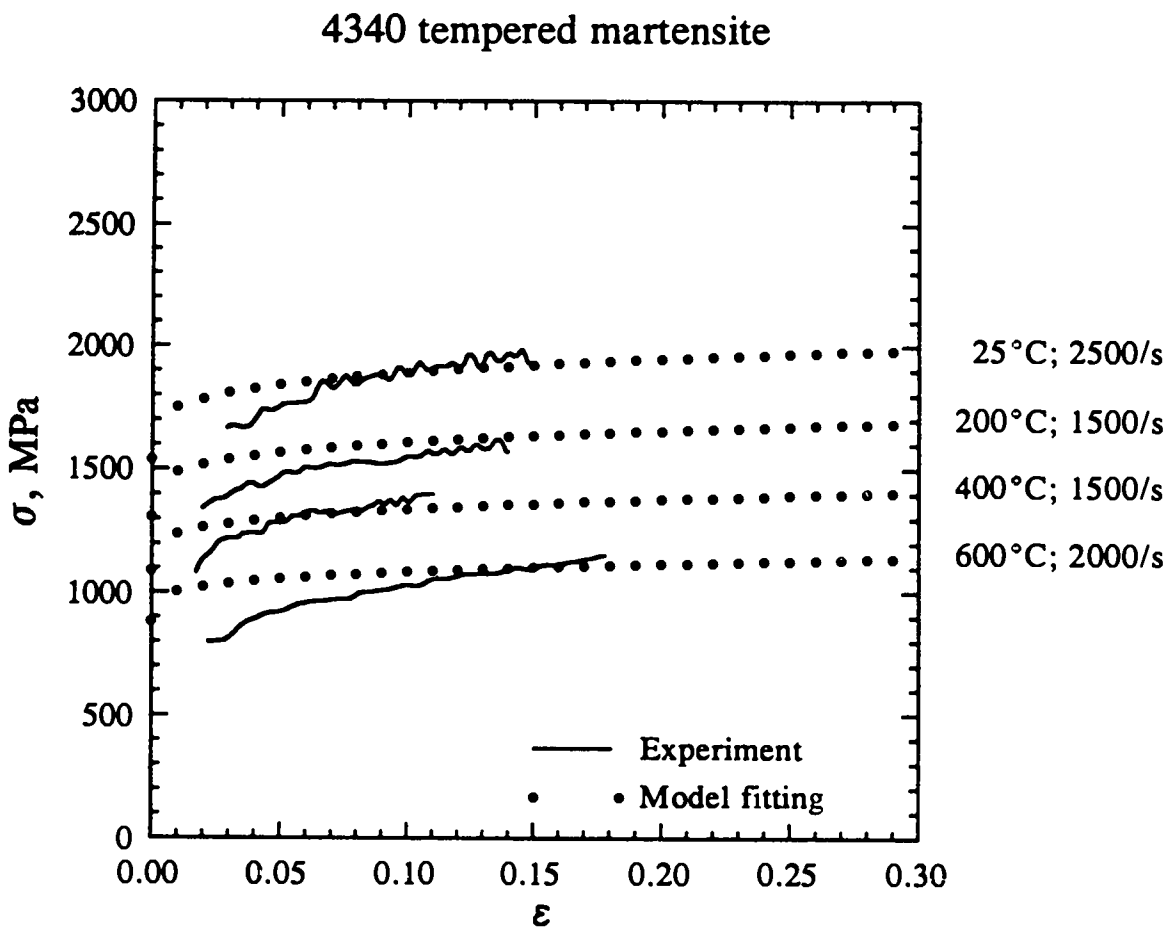

Johnson-Cook Model:

$$\sigma = (A + B\varepsilon^{n})(1 + C\ln\dot{\varepsilon}^{*})(1 - ((T - T_{ROOM})/(T_{MELT} - T_{ROOM}))^{m})$$

Using constants derived by Johnson & Holmquist for their High Hard Armor :

A=1504 MPa B=569 MPa n=0.22

C=0.003 but m=0.90 instead of 1.17 T_m=1783 K

Figure 34. Data from Figure 32 fit by changing m from 1.17 to 0.90.

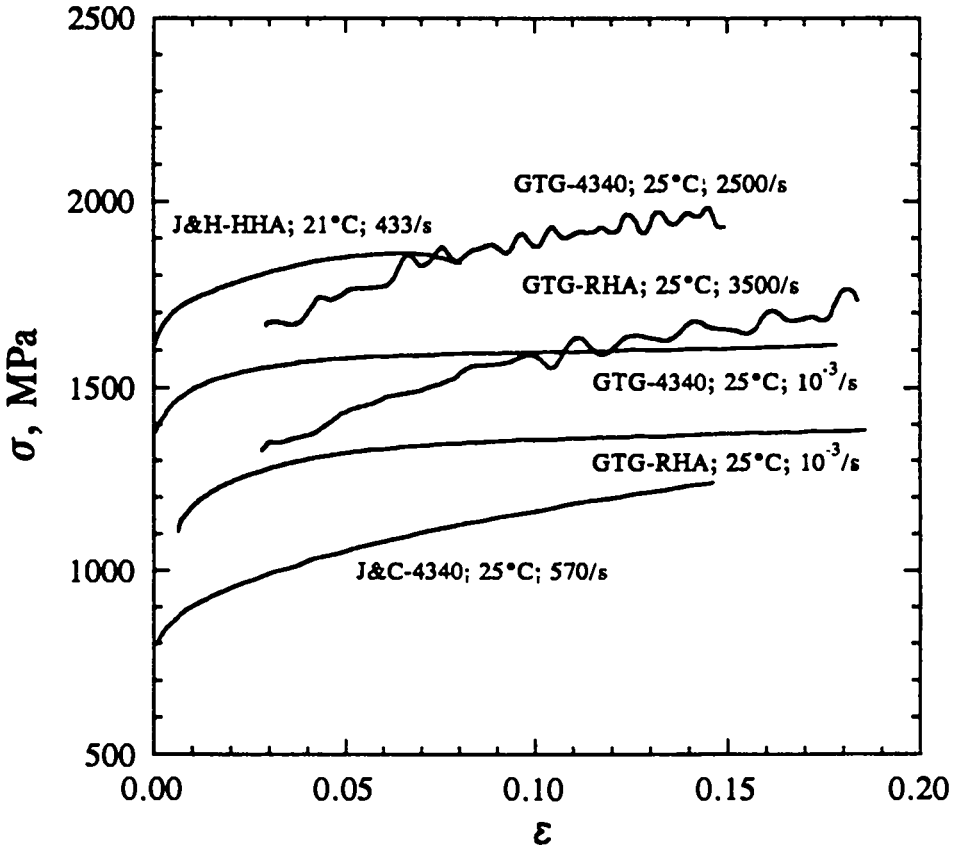

Figure 35. Plot of four different steels on the same axis for comparison. Note that the curve fitting matches only the low strain rate, room temperature data reasonably well.

Appendix A

Appendix A consists of figures A-1 through A-6, which present the raw data for Los Alamos 4340 tempered martensite, RHA steel, tantalum, OFE copper, AL-7039, and Al-5083.

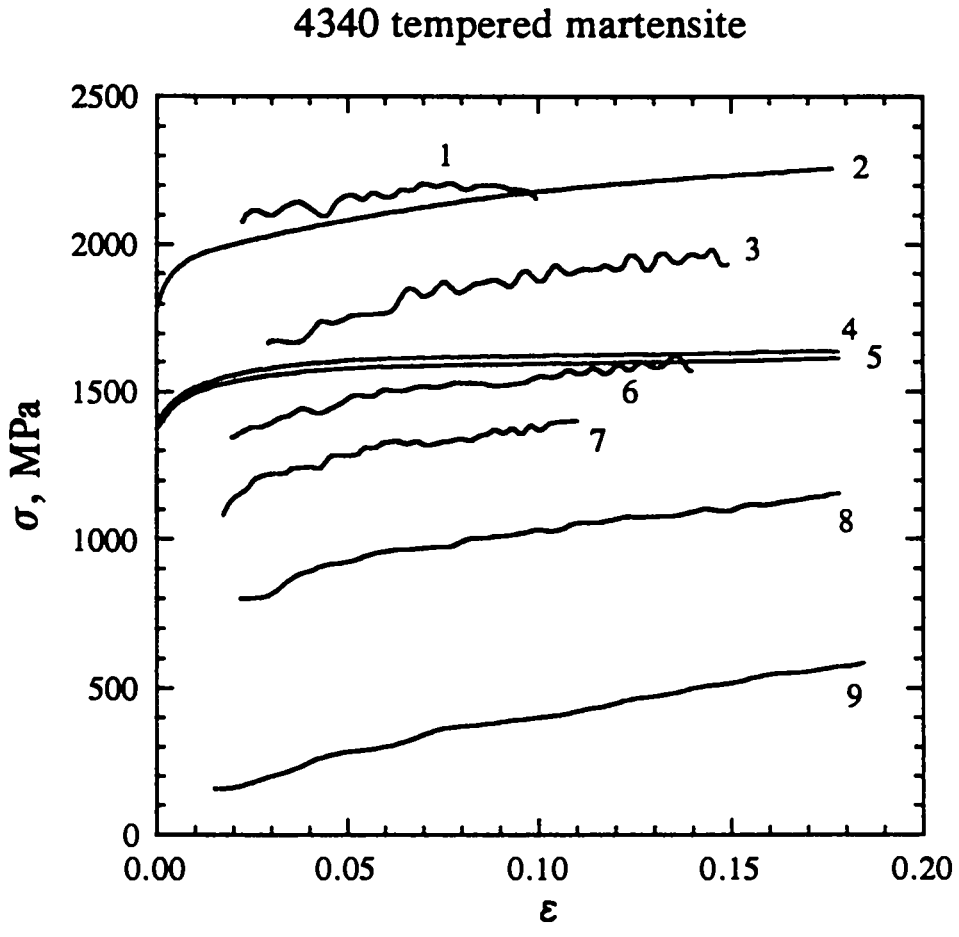

1: -196°C; 2000/s

2: -196°C; 0.001/s

3: 25°C; 2500/s

4: 25°C; 0.1/s

5: 25°C; 0.001/s

6: 200°C; 1500/s

7: 400°C; 1500/s

8: 600°C; 2000/s

9: 800°C; 4000/s

Figure A-1. Raw data for Los Alamos 4340 tempered martensite.

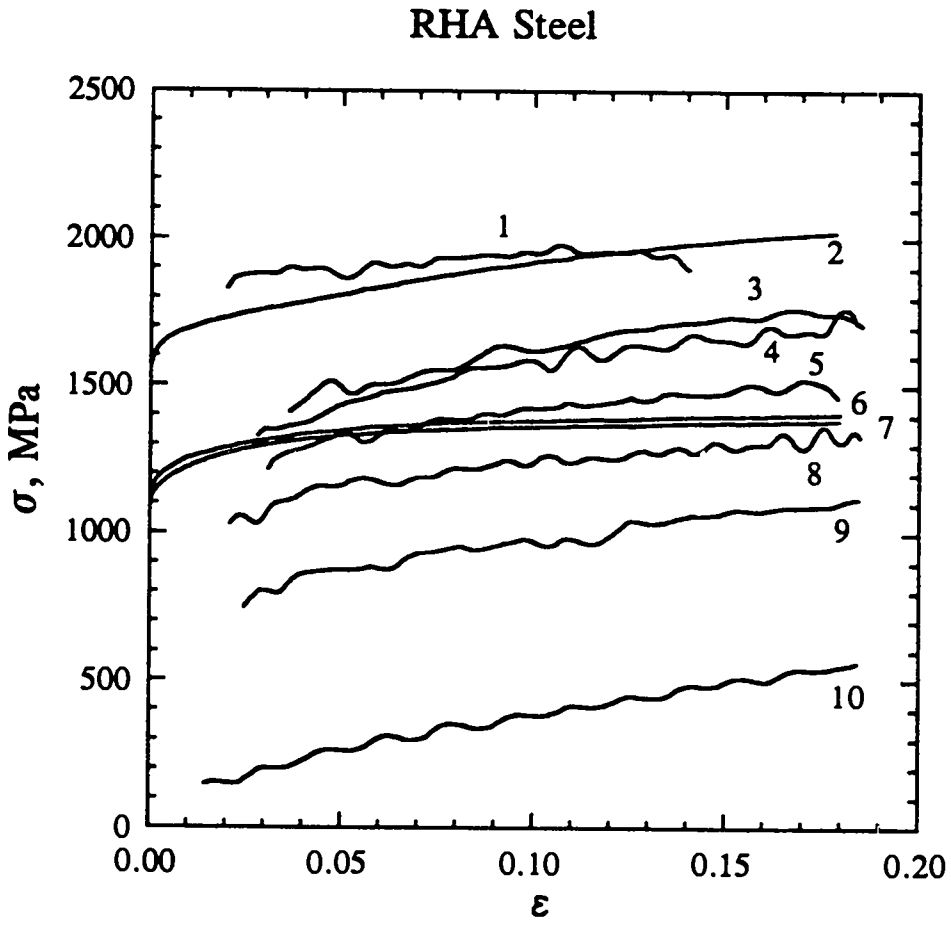

1: -196°C; 2500/s

2: -196°C; 0.001/s

3: 25°C; 7000/s

4: 25°C; 3500/s

5: 200°C; 3000/s

6: 25°C; 0.1/s

7: 25°C; 0.001/s

8: 400°C; 3000/s

9: 600°C; 3500/s

10: 800°C; 4500/s

Figure A-2. Raw data for RHA steel.

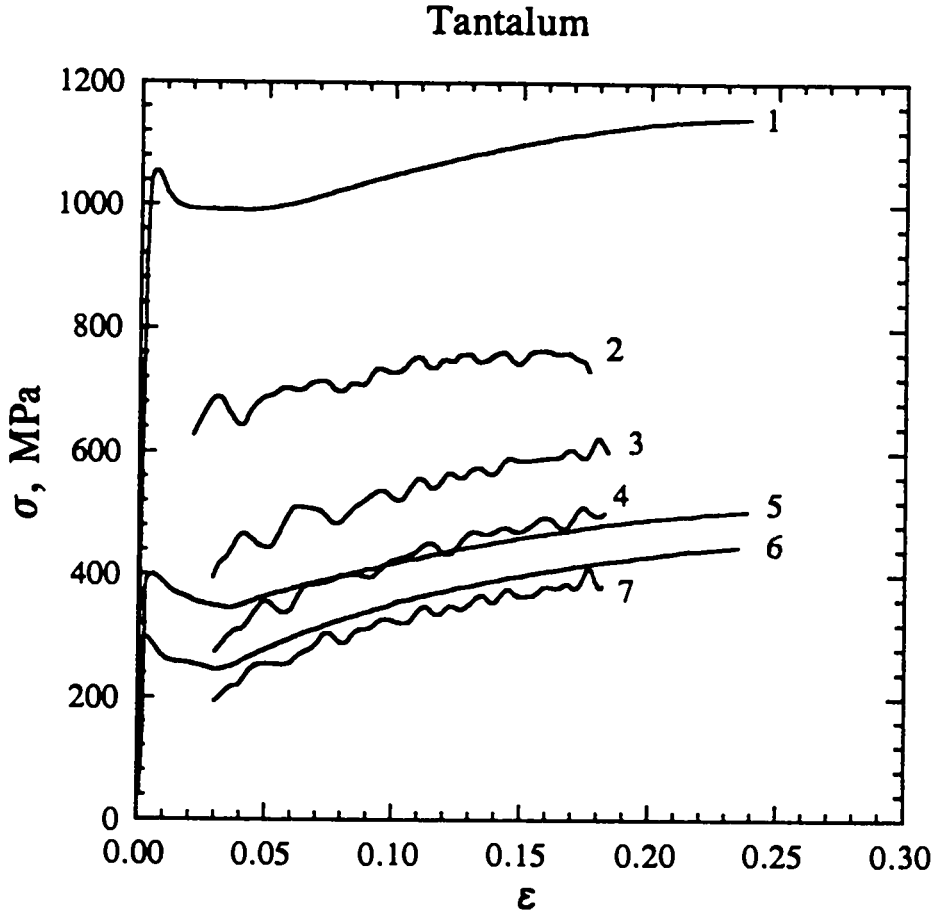

1: -196°C; 0.001/s

2: 25°C; 3000/s

3: 200°C; 3000/s

4: 400°C; 4000/s

5: 25°C; 0.1/s

6: 25°C; 0.001/s

7: 1000°C; 3000/s

Figure A-3. Raw data for tantalum.

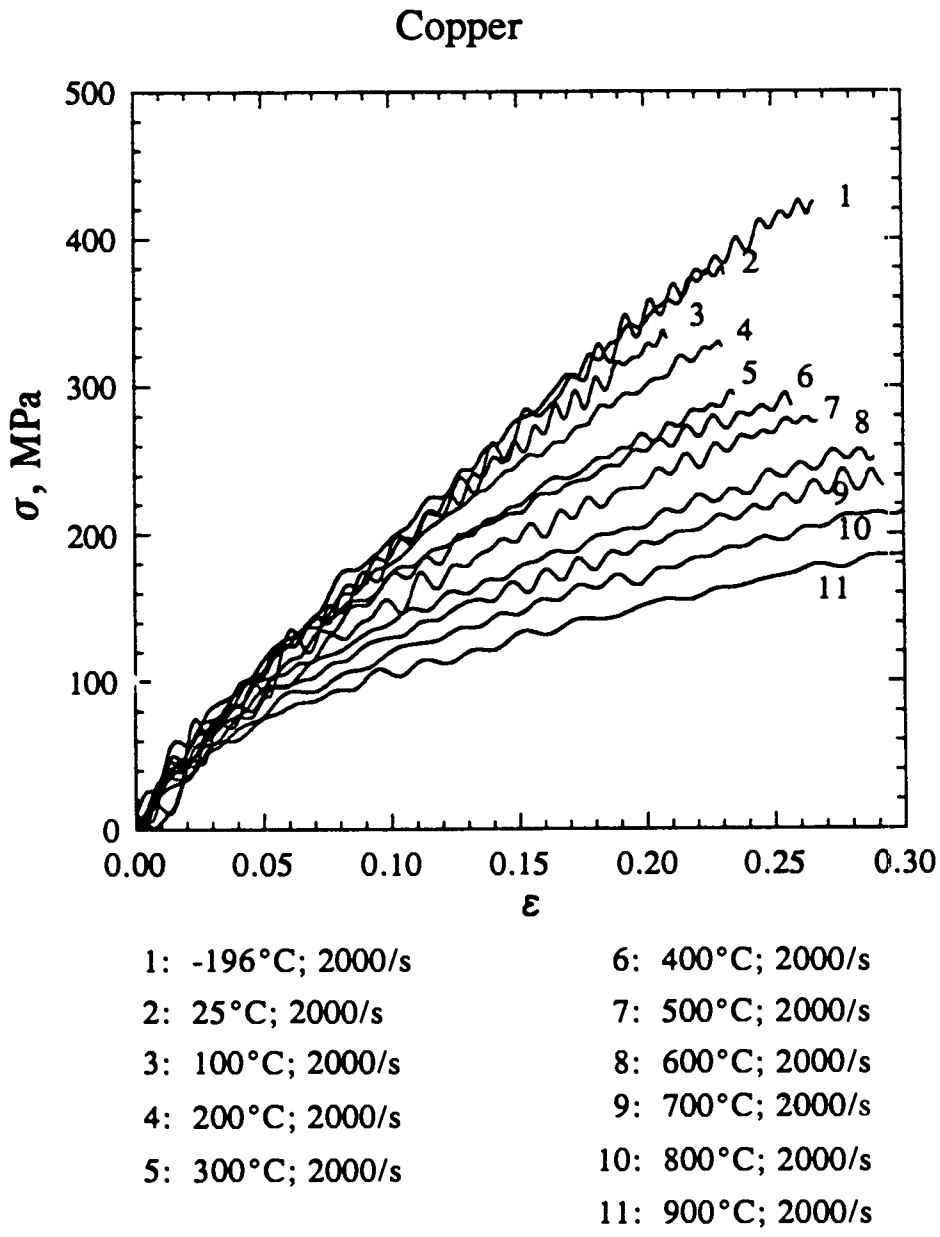

Figure A-4. Raw data for OFE copper.

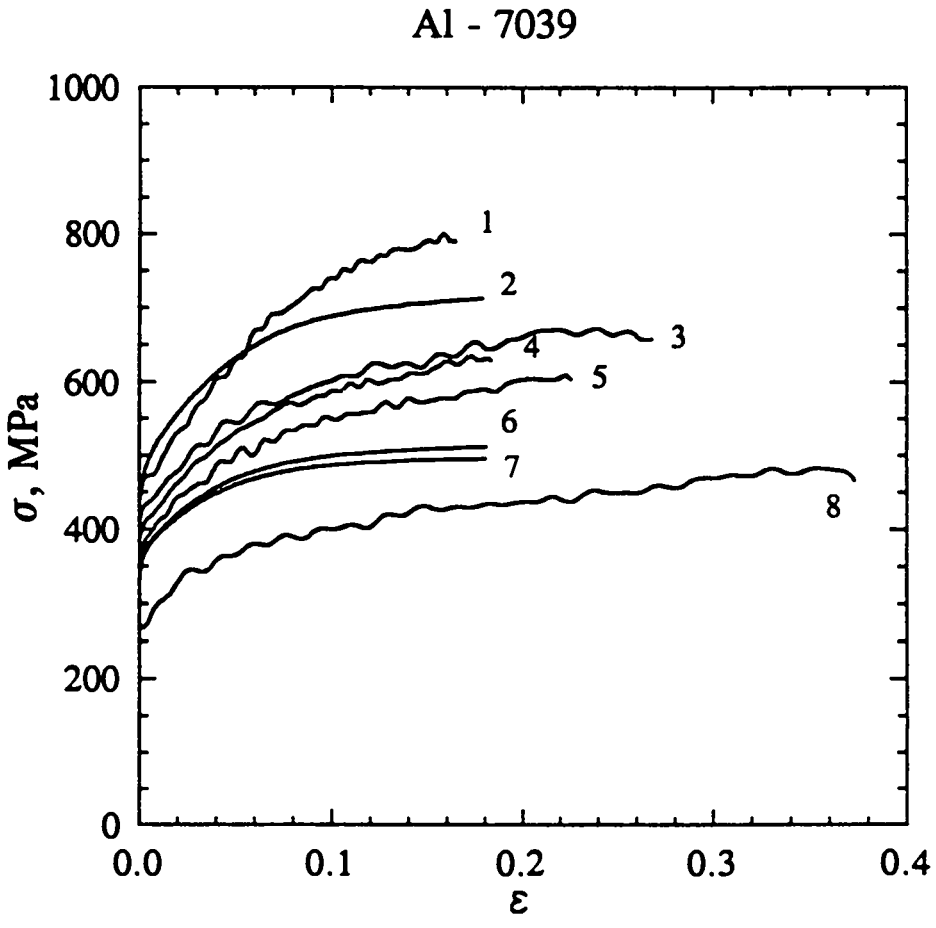

1. -196°C; 2000/s
2. -196°C; 0.001/s
3. 25°C; 6000/s
4. 25°C; 2000/s
5. 100°C; 2500/s
6. 25°C; 0.1/s
7. 25°C; 0.001/s
8. 200°C; 4000/s

Figure A-5. Raw data for Al-7039.

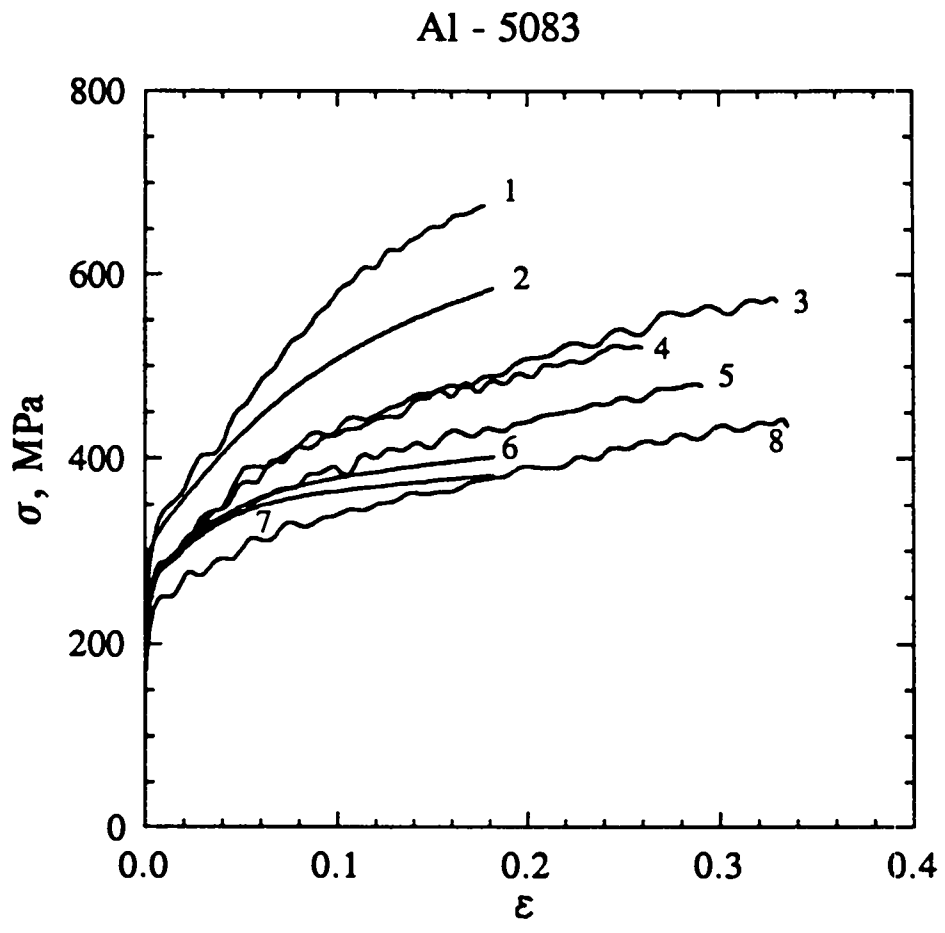

1. -196°C; 2000/s
2. -196°C; 0.001/s
3. 25°C; 7000/s
4. 25°C; 2500/s
5. 100°C; 3000/s
6. ***25°C; 0.001/s***
7. ***25°C; 0.1/s***
8. 200°C; 3500/s

Figure A-6. Raw data for Al-5083.

Appendix B

We wrote this report in an unclassified fashion so that it can be given wide distribution among the computational community. Users may question the type or the pedigree of the materials used to obtain the data. The information in this Appendix (Figures B-1 through B-4) is included to establish the credentials of the materials characterized. We feel that what is represented in this report is close to the characteristics of the metallic materials used in current armors.

Three generic materials are included in the report—copper, tantalum, and 4340 steel. The 4340 steel was homogenized at temperature, quenched, and heat treated at Los Alamos to Brinnell hardness 360. The hardness was uniform across the surface; thus this is an idealized specimen. The analyses for all three generic materials are included below.

The request for steel and aluminum armor specimens was made to the manufacturers of the M1A2 tank and the Bradley Fighting Vehicle. The specimens of RHA from the Warren, MI tank plant were lost in shipping so we obtained a piece of RHA from the principle supplier of RHA to manufacturers in the U.S., Heflin Steel Co. of Phoenix, AZ. No further heat treatment was given this specimen before the strain rate tests were conducted. Test samples were carefully removed from the material in such a way as not to alter the heat treat of the RHA. Samples were taken both perpendicular and parallel to the rolling direction. Data presented are a composite of all of the measured data analyzed as described in the figure caption.

Samples of aluminum were taken directly from the assembly line at FMC Corporation in San José, CA. These were supplied in one inch thick sections as cutoffs from the material used in the assembly of BFVs. We felt that the aluminum was an appropriate representation of the vehicle armor and already homogenized, so samples were cut perpendicular to the large surfaces. The MIL specification requirements are included in this Appendix.

DELIVERY COPY

PHONE (602)272-0461

EARLE M. JORGENSEN CO.
STEEL

5445 W MADISON ST
P.O. BOX 6737
PHOENIX, AZ 85005

DUNS NUMBER?

SALES UNIT	SHIP UNIT	INVOICE NUMBER	TR
P	L	021249	CT

CUSTOMER ORDER - REQ. NO.	DATE ENTERED	BY	ORDERED BY	
7-NSE-8447-J-1	09/17/86	BILL	DOROTHY	RESALE

SOLD TO: UNIVERSITY OF CALIFORNIA
LOS ALAMOS SCIENTIFIC LAB
P O BOX 1663
LOS ALAMOS NM 87544

SHIP TO: RECEIVING DEPT
SM 30 WAREHOUSE
BIKINI ROAD 87545
LOS ALAMOS NM

LEP

	DESCRIPTION & SPECIFICATIONS	SIZE	
CREUSOT R-6107 VS	E-4340 HR ANN PLATE AMS 6359-D AMS 2301	5/8" TH We certify to the best of our knowledge this material is free from Mercury and Radium Contamination	NO

CHEMICAL ANALYSIS

HEAT NO.	C	MN	PHOS	SUL	SIL	NI	CR	CU	MO	N	G/S	AMS 2301 P	AMS 2301 S
36312	.405	.696	.0108	.0002	.248	1.870	.851	.178	.233		8/9	0	0

MECHANICAL PROPERTIES

YIELD THOUSAND LBS/SQ. IN.	TENSILE STRENGTH THOUSAND LBS/SQ. IN.	ELONG. % IN 2"IN	RED. OF AREA	BRINELL	ROCKWELL B	BEND	EMB	MACRO	MICRO	DECARB
					93/95	OK				

NYDRO	FLATTENING	FLARING	FLANGE	MAG

END-QUENCH HARDENABILITY

1	4	5	6	8	9
			55.5		

10	12	16	20	24	32
			51		

DEVELOPED HARDNESS

We hereby certify that the material covered by this report has been inspected in accordance with, and has been found to meet, the requirements described herein, including any specifications forming a part of the description, and test results are on file subject to examination.

SUBSCRIBED AND SWORN TO BEFORE ME

363/12 — 85

OFFICIAL SEAL
CHARLES E. CHASE
NOTARY PUBLIC - CALIFORNIA
LOS ANGELES COUNTY
My Commission Expires June 26, 1987

MY COMMISSION EXPIRES

CERTIFIED MATERIAL TEST REPORT
EARLE M. JORGENSEN CO.

BY _____
STOCK RECORDS SUPERVISOR

FORM 91-A (1986)

Figure B-1. Specification sheet for 4340 steel from Earle M. Jorgensen Co. The plate was fully annealed by heating at 1000°C for 15 hours followed by cooling to 500°C at 3°C/hr. After this it was air-cooled to room temperature. It was then reheated to 825°C for 15 min, quenched in oil, tempered at 400°C for 2 hours, and allowed to air cool. Sections of the plate were cut perpendicular to and along the rolling axis for strain measurements.

LUKENS STEEL 005095 — A LUKENS COMPANY

TEST CERTIFICATE

FILE NO 3326-31-02
DATE 06/05/90
MILL ORDER NO 10585-001

CUSTOMER P.O. 15172
DESCRIPTION 2 -' 5 -X- 74 -X- 74 RECTANGLE 03-C

SOLD TO	SEND TO	SHIP TO
HEFLIN STEEL SUPPLY CO.	HEFLIN STEEL SUPPLY CO.	HEFLIN STEEL SUPPLY CO.
P.O.BOX 1249	P.O.BOX 1249	C/O DESERT-WILKERSON
		SPRR SPUR 3972
PHOENIX AZ 85001	PHOENIX AZ 85001	PHOENIX, AZ 85001

THIS MATERIAL HAS BEEN MANUFACTURED AND TESTED IN ACCORDANCE WITH PURCHASE ORDER REQUIREMENTS AND SPECIFICATIONS

MIL R-12560G(MR) CL 1 YR 89 AMEND 3

COPY

MELT/SLAB	C	MN	P	S	CU	SI	NI	CR	MO	V	TI	B	AL	ZR	SB	AS	PRACTICES
86326 /4																	VTP E/F QUALITY
86326	.25	.22	.010	.005	.14	.22	3.08	1.43	.23		.002	.0001	.021	.005	.0050	.0060	
PROD ANALYSIS	.26																

TENSILES / CHARPY V IMPACTS — FULL

TYPE	YIELD PSI X 100	TENSILE PSI X 100	% ELONG IN	% R.A.	TYPE	TEMP	FT LBS			MILS LATERAL EXPANSION	% SHEAR
					TL	-40	48	50	53		
					TX	-40	46	48	51		

OTHER TESTS PERFORMED

BRINELL - 262 262 TEST LOC-T
BRINELL - 262 269 TEST LOC-B

INFORMATION

WEIGHT PER PIECE = 7765
ALL TEMPERATURES APPEAR IN DEGREES FAHRENHEIT.
FIRING RECORD = 3AR 90000846 BALLISTIC TEST ACCEPTED.
IMPACTS TAKEN FROM SLAB 4 BRINNEL = 263
PRODUCED IN ACCORDANCE WITH INSPECTION REQUIREMENTS
OF MIL-I-45208A

SK 86130 WO 8967
NAME Univ. of CA
CUST. PO 2KR3-H9812-1
Quality Assurance
HEFLIN STEEL CO.

APPROVED
HEFLIN STEEL CO.
JUN 19 1990
QUALITY ASSURANCE MGR

HEAT TREAT CYCLES - MATL OR TESTS - DEG F.

MATL	TEST	NOM TEMP	MIN TEMP	MAX TEMP	HOLD MINS	COOL METHOD	END TEMP
X	X	1650			0190	WQ	
X	X	1160			0390	WQ	

HEAT TREAT CYCLES - TESTS ONLY - DEG F.

START END TEMP	NOM TEMP	MIN TEMP	MAX TEMP	HOLD MINS	HEAT RATE MAX	COOL RATE MAX

WE HEREBY CERTIFY THE ABOVE INFORMATION IS CORRECT: Quality Assurance Laboratory, Coatesville, PA 19320

Figure B-2. Specification sheets for the rolled homogeneous armor (RHA) supplied by Heflin Steel Co.

LUKENS STEEL
A LUKENS COMPANY

TEST CERTIFICATE

CUSTOMER PO 15172
DESCRIPTION: 2 ÷ 5 ¬X- 74 ¬X÷ 74 RECTANGLE

DATE 06/05/90
MILL ORDER NO 10585-001

SOLD TO:	SEND TO: 03-C	SHIP TO:
HEFLIN STEEL SUPPLY CO. P.O.BOX 1249	HEFLIN STEEL SUPPLY CO. P.O.BOX 1249	HEFLIN STEEL SUPPLY CO. C/O DESERT-WILKERSON SPAR SPUR 8972
PHOENIX AZ 85001	PHOENIX AZ 85001	PHOENIX. AZ 85001

THIS MATERIAL HAS BEEN MANUFACTURED AND TESTED IN ACCORDANCE WITH PURCHASE ORDER REQUIREMENTS AND SPECIFICATIONS

MIL A-12560G(MR) CL 1 YR 89 AMEND3

MELT/SLAB	C	MN	P	S	CU	SI	NI	CR	MO	V	TI	B	SN	PB			PRACTICES
B6326 /4																	
B6326													.015	.001			

TENSILES					CHARPY V IMPACTS						OTHER TESTS PERFORMED
TYPE	YIELD PSI X 100	TENSILE PSI X 100	% ELONG IN	% R.A.	TYPE	TEMP			MILS LATERAL EXPANSION		% SHEAR	

INFORMATION	HEAT TREAT CYCLES - MATL OR TESTS - DEG F.							
	MATL	TEST	NOM TEMP	MIN TEMP	MAX TEMP	HOLD MINS	COOL METHOD	END TEMP

HEAT TREAT CYCLES - TESTS ONLY - DEG F.						
START END TEMP	NOM TEMP	MIN TEMP	MAX TEMP	HOLD MINS	HEAT RATE MAX	COOL RATE MAX

WE HEREBY CERTIFY THE ABOVE INFORMATION IS CORRECT

Quality Assurance Laboratory
Centerville, PA 15301

Figure B-2, continued.

(011/001)

LUKENS STEEL COMPANY

Q.A. — INSPECTION DEPARTMENT

NON DESTRUCTIVE TESTING REPORT

CUSTOMER: Heflin Steel AZ	MILL ORDER NO: 3526-10585	SPECIFICATION/PROCEDURE: A 578-85-100% [illegible] — DATE: 5-22-90
CUSTOMER NO: 15772	QUALITY: [illegible]	NO PCS: 1 — GAUGE: 5 — WIDTH: 74 — LENGTH: 74
INSPECTOR'S NAME (LEVEL) SNT TC 1A): Book	WITNESSED BY:	MELT & SLAB: B6326-4 — MARK NO: GG-2 — ITEM NO: 1

UT ☑ SB ☑ AB ☐ — EQUIPMENT USED: [illegible] 8 7-18-90	MT ☐ — EQUIPMENT USED:	PT ☐ — EQUIPMENT USED:
TRANSDUCER: [illegible]	TYPE OF PRODS:	METHOD:
SIZE & FREQ: 1¼ dia 2.25 MHZ	SPACING:	
COUPLANT: [illegible]	GRID REF:	
METHOD: [illegible]	AMPERAGE:	
AMPLITUDE: 80% — GRID PIT: 100% — TYPE OF SURFACE: Blasted	METHOD: — TYPE OF SURFACE: — IPV ☐	TYPE OF SURFACE:

T (Top)

C

UT ok per Spec

[illegible signature] 5-23-90

INSPECTOR (SUPERVISOR LEVEL) SNT TC 1A)

Figure B-2, continued.

Form No. 81A (8/11/89)

LUKENS STEEL COMPANY

Q.A. — INSPECTION DEPARTMENT

NON DESTRUCTIVE TESTING REPORT

CUSTOMER	MILL ORDER NO 3526-10585	SPECIFICATION/PROCEDURE A578-85-100% Scanning (S) Mod To 12"			DATE 5-21-90
CUSTOMER NO 15172	QUALITY Mil-A-12560H(MR) 89-1 Amend #3	NO PCS 1	GAUGE 5"	WIDTH 74	LENGTH 74
INSPECTOR'S NAME & LEVEL (SNT TC 1A) Burk	WITNESSED BY	MELT & SLAB B6332C-4		MARK NO PQ #3 ITEM NO 1	

UT / STRAIGHT BEAM — EQUIPMENT USED: Mk 1 8 7-13-90	MT — EQUIPMENT USED	PT — EQUIPMENT USED
TRANSDUCER Aerotech	TYPE OF PRODS	METHOD
SIZE & FREQ 1⅛" dia 2.25 MHZ	SPACING	
COUPLANT 3+W	GRID REF	
METHOD Cont	AMPERAGE	
AMPLITUDE 80% — TYPE OF SURFACE Cond	METHOD — TYPE	TYPE OF SURFACE
GRID REF 100%	TYPE OF SURFACE	

T (Feet)

C

Ut ok per Spec.

[illegible] 5-21-90

[illegible]

Figure B-2, continued.

Chemical Composition of
Copper, Tantalum A, 4340 Steel, RHA Steel, Al-5083, and Al-7039

	Sample Composition in					
Element	Cu in wt %	Ta in ppm	4340 Steel in wt %	RHA in wt %	Al-5083 in wt %	Al-7039 in wt %
C		9	.405	.25		
N		18				
O		44				
H		<1				
Fe		<5	major	major	.40 max	.40 max
Ni		<5				
Cr		<5	.851	1.43	.05–.25	.15–.25
W		<150				
Nb		123				
Tc		balance				
P			.0108	.010		
S			.0002	.005		
Mo			.233	.23		
B				.0001		
Zr				.005		
Sb				.0050		
As				.0060		
Sn				.015		
Pb				.001		
Si			.248	.22	.40 max	.30 max
Cu	99.99*		.178	.14	.10 max	.10 max
Mn			.696	.22	.40–1.0	.10–.40
Mg					4.0–4.9	2.3–3.3
Zn					.25 max	3.5–4.4
Ti				.002	.15 max	.10 max
Others, Each					.05	.05 max
Others, Total					.15	.15 max
Al				.021	remainder	remainder

* Remainder must meet ASTM B170 standards.

Figure B-3. Chemical composition of copper, tantalum, 4340 Steel, RHA Steel, Al-5083, and Al-7039.

Mechanical Properties of
Copper, Tantalum A, 4340 Steel, RHA Steel, Al-5083, and Al-7039

	Mechanical Properties				
Sample	Thickness	Tensile Strength, psi	UTS	Elongation, %	Notes
Cu	n/a	45,000	40,000	20	The copper is oxygen-free copper, made from plate stock. Electrolytic copper was annealed at 600°C for 1 hour and cooled to room temperature in vacuum. The microstructure exhibited equiaxed grains of approx 50 μm average size.
Ta	5 mm	30,000	n/a	n/a	The tantalum used in other tests at Los Alamos was supplied in as annealed plate and contained equiaxed grains of approx 45 μm average size.
4340 Steel	n/a	200,000–210,000	192,000–198,000	10–11	4340 plate was fully annealed by heating at 1000°C for 15 hours, followed by cooling to 500°C at 3°C/hr. After this it was air-cooled to room temperature. It was then reheated to 825°C for 15 min, quenched in oil, tempered at 400°C for 2 hours, and allowed to air cool. Sections of the plate were cut perpendicular to and along the rolling axis for strain measurements.
RHA Steel	n/a	150,000	135,000	18	n/a
Al-7039	up to 1.5 in.	60,000	51,000	9	Al-7039 plate was obtained from FMC in San José, CA, directly from the manufacturing line for the Bradley Fighting Vehicle. The 1-in.-thick sample was "cut off" directly from the fabrication line.
	<1.5 in.	57,000	48,000	8	
Al-5083	.25–.499 in.	45,000	35,000	8	Al-5083 plate was obtained from FMC in San José, CA, directly from the manufacturing line for the Bradley Fighting Vehicle. The 1-in.-thick sample was "cut off" directly from the fabrication line.
	.5–up to 2.00 in.	45,000	37,000	8	
	2.00–3.00 in.	44,000	35,000	9	

Figure B-4. Mechanical Properties of Copper, Tantalum A, 4340 Steel, RHA Steel, Al-5083, and Al-7039.

Los Alamos
NATIONAL LABORATORY
Los Alamos, New Mexico 87545